PuHSFA4a Enhances Tolerance To Excess Zinc by Regulating Reactive Oxygen Species Production and Root Development in *Populus*[1][OPEN]

Haizhen Zhang,[a] Jingli Yang,[a] Wenlong Li,[a] Yingxi Chen,[a] Han Lu,[a] Shicheng Zhao,[b] Dandan Li,[a] Ming Wei,[a] and Chenghao Li[a,2,3]

[a]State Key Laboratory of Tree Genetics and Breeding, Northeast Forestry University, Harbin 150040, China
[b]School of Pharmacy, Harbin University of Commerce, Harbin 150028, China

ORCID ID: 0000-0003-0916-0409 (C.L.).

Zinc (Zn) is an essential micronutrient but in excess is highly toxic to plants. Plants regulate Zn homeostasis and withstand excess Zn through various pathways; these pathways are generally tightly regulated by a specific set of genes. However, the transcription factors involved in excess Zn tolerance have yet to be identified. Here, we characterized a *Populus ussuriensis* heat shock transcription factor A4a (PuHSFA4a) that acts as a positive regulator of excess Zn tolerance in *P. ussuriensis*. We used overexpression (*PuHSFA4a*-OE) and chimeric dominant repressor (*PuHSFA4a-SRDX*) lines to identify the targets of *PuHSFA4a*. *PuHSFA4a* transcription is specifically induced in roots by high Zn. Overexpression of *PuHSFA4a* conferred excess Zn tolerance and a dominant repressor version of *PuHSFA4a* increased excess Zn sensitivity in *P. ussuriensis* by regulating the antioxidant system in roots. PuHSFA4a coordinately activates genes related to abiotic stress responses and root development and directly binds to the promoter regions of glutathione-s-transferase U17 (*PuGSTU17*) and phospholipase A_2 (*PuPLA*$_2$). *PuGSTU17* overexpression significantly increased GST activity and reduced reactive oxygen species levels in roots while *PuGSTU17*-RNA interference lines exhibited the opposite phenotype. Furthermore, *PuPLA*$_2$ overexpression promoted root growth under high Zn stress. Taken together, we provide evidence that *PuHSFA4a* coordinately activates the antioxidant system and root development-related genes and directly targets *PuGSTU17* and *PuPLA*, thereby promoting excess Zn tolerance in *P. ussuriensis* roots.

Zinc (Zn) is an essential micronutrient but its excess in soil is highly toxic to plants (Broadley et al., 2007; Wang et al., 2009). To cope with Zn toxicity, plants have evolved complex adaptive responses to allow them to tolerate, acclimate to, or avoid excess Zn stress (Lin and Aarts, 2012; Schvartzman et al., 2018). Numerous studies have shown that, after exposure to stress due to the presence of excess Zn, the expression levels of many genes significantly increase or decrease, indicating that transcriptional reprogramming plays an important role in adaptive responses to Zn stress (Lin and Aarts, 2012; Luo et al., 2016).

At the cellular level, high Zn accumulation induces oxidative stress by producing reactive oxygen species (ROS). Elevated ROS levels create a strongly oxidizing environment, causing membrane lipid peroxidation and activating signaling pathways that lead to cell death (Lin and Aarts, 2012). Plants respond to such stresses by activating antioxidant enzymes (Wang et al., 2009). In tomato (*Solanum lycopersicum*), increased ascorbate peroxidase (APX) activity eliminates H_2O_2 caused by Zn accumulation in the roots (Xu et al., 2008). Another study in green bean (*Phaseolus vulgaris*) found that enhanced glutathione reductase activity in leaves may be a response to Zn-induced oxidative stress (Chaoui et al., 1997). Similarly, the enzymes glutathione-s-transferase (GST) and glutathione peroxidase use glutathione as a substrate to detoxify H_2O_2 and sequester Zn by acting as a precursor for synthesis of phytochelatins (Garg and Kaur, 2013). In addition, several genes have been shown to be involved in excess Zn detoxification. These include: Arabidopsis (*Arabidopsis thaliana*) *AtHMA4* (Verret et al., 2004) and *AtMTP1* (Desbrosses-Fonrouge et al., 2005), rice (*Oryza sativa*) *OsHMA2* (Takahashi et al., 2012) and *OZT1* (Lan et al., 2013), *Saccharomyces cerevisiae ZRC1* (Miyabe et al., 2001), *Populus alba AQUA1* (Ariani et al., 2016),

[1]This work was sup\ported by the Fundamental Research Funds for the Central Universities of China (2572018CL04 to C.L.), the 111 Project (B16010 to C.L.), Fundamental Research Funds for the Central Universities of China (2572015AA20 to H.Z.), and the National Natural Science Foundation of China (31400573 to J.Y.).

[2]Author for contact: chli@nefu.edu.cn.
[3]Senior author.
The author responsible for distribution of materials integral to the findings presented in this article in accordance with the policy described in the Instructions for Authors (www.plantphysiol.org) is: Chenghao Li (chli@nefu.edu.cn).

C.L., J.Y., and H.Z. designed and conceived the experiments; H.Z., W.L., Y.C., S.Z., D.L., and M.W. performed experiments; H.Z. and H.L. analyzed data; C.L. and H.Z. wrote the article; all authors reviewed, revised, and approved the article.

[OPEN]Articles can be viewed without a subscription.
www.plantphysiol.org/cgi/doi/10.1104/pp.18.01495

and cyanobacteria (*Synechococcus* PCC 7942) *SmtA* (Xu et al., 2010). Moreover, in both *Drosophila* and humans (*Homo sapiens*), the Zn finger transcription factor (TF) metal-responsive TF-1 appears to confer excess Zn tolerance (Laity and Andrews, 2007). Although these studies have identified many genes involved in Zn detoxification and tolerance, the TFs that regulate the mechanisms of Zn detoxification have not yet been characterized in plants.

Heat shock transcription factors (HSFs) regulate the transcription of genes related to heat and other abiotic stresses (von Koskull-Döring et al., 2007). HSFs are divided into three categories—A, B, and C—based on their structures. HSFA4, a class A HSF, is found in a variety of plant species and confers tolerance to certain environmental stresses. For example, estradiol-dependent induction of Arabidopsis *AtHSFA4a* confers enhanced tolerance to salt and oxidative stress by interacting with MPK3/MPK6 signaling (Pérez-Salamó et al., 2014). Overexpression of *CmHSFA4* enhances salt tolerance by regulating Na^+/K^+ ion and ROS homeostasis in *Chrysanthemum* (Li et al., 2018). Ectopic overexpression of *Brassica napus BnHSFA4a* in Arabidopsis improved desiccation tolerance (Lang et al., 2017). Overexpression of wheat *TaHSFA4a* conferred cadmium (Cd) tolerance and rice *OsHSFA4a* knockouts showed Cd hypersensitivity (Shim et al., 2009). However, to date no studies have assessed whether HSF TFs are involved in regulating tolerance to excess Zn stress.

The genus *Populus* (*Populus* spp) comprises deciduous hardwood trees that are mainly distributed in the northern hemisphere. *Populus* has been recognized as a suitable tree for phytoremediation due to its rapid growth, high biomass, extensive root system, and ease of propagation (Luo et al., 2016). Some studies have performed transcriptomic analysis and genetic manipulation to examine the molecular mechanisms responsible for Cd, copper (Cu), and Zn remediation in *Populus* species, including *Populus euphratica* (Han et al., 2014), *Populus trichocarpa* × *deltoides* (Kohler et al., 2004), *Populus canescens* (Luo et al., 2016), and *Populus nigra* (Bittsánszky et al., 2005). *Populus* spp have been reported to uptake several inorganic pollutants including Zn, but their capacity for heavy metal tolerance may be capable of further improvement (Bittsánszky et al., 2005).

The forested areas in the northeast of China are rich in Zn mineral resources. Years of mining activities have caused the destruction of surface vegetation near Zn mines in these regions (Hu et al., 2013). *Populus ussuriensis*, belonging to *Populus* sect. *Tacamahaca* in the *Salicaceae*, is a unique tree species native to the forested regions of northeastern China. It is one of the fastest growing tree species—especially in the young forest stage of forest succession—and is thus one of the main tree species used for forest renewal in parts of northeastern China (Su et al., 2001). Thus, *P. ussuriensis* is an excellent candidate for forest restoration in former Zn mining areas in northeastern China. In this study, we characterized PuHSFA4a, a *P. ussuriensis* TF belonging to the Class A4a subgroup of the HSF family. We demonstrate that PuHSFA4a specifically confers tolerance to excess Zn in transgenic *P. ussuriensis*. We also provide evidence that PuHSFA4a affects antioxidant scavenging and root development-related gene expression by directly targeting *PuGSTU17* to eliminate ROS in roots and $PuPLA_2$ (*phospholipase A*) to promote root growth under excess Zn. This study improves our understanding of the physiological and molecular responses to Zn exposure in *Populus* roots.

RESULTS

PuHSFA4a Is Specifically Induced in Roots by Excess Zn

The expression profiles of *P. ussuriensis* Class A HSF genes in response to abiotic stress were investigated using reverse transcription quantitative PCR (RT-qPCR). Among the Class A *PuHSF* genes assessed, only *PuHSFA4a* was substantially upregulated specifically in roots in response to high Zn stress (Fig. 1A; Supplemental Fig. S1A). The expression of *PuHSFA4a* was higher in roots than in leaves under control conditions (Fig. 1A). The expression level of *PuHSFA4a* in roots did not significantly increase in response to Cd, Cu, iron (Fe), PEG6000, abscisic acid (ABA), and NaCl stresses. (Supplemental Fig. S1B).

Next, the 2,203-bp *PuHSFA4a* promoter was fused to the *GUS* (*uidA*) gene, and the ProPuHSFA4a::*GUS* construct was transformed into *P. ussuriensis*. No GUS activity was observed under normal culture conditions (Fig. 1B). However, under high Zn stress, strong GUS activity was detected in whole roots but not in shoots (Fig. 1B). These observations suggest that *PuHSFA4a* functions specifically in root in response to high Zn stress.

Cloning and Sequence Characterization of *PuHSFA4a*

The full-length *PuHSFA4a* gene was obtained from *P. ussuriensis*. Phylogenetic analysis was performed on PuHSFA4a and similar HSFA4a proteins found in other plant species. The results of these comparisons showed that PuHSFA4a belongs to the HSF ClassA4a subgroup, where it clustered with AtHSFA4a, BnHSFA4a, MsHSFA4a, CmHSFA4a, OsHSFA4a, and TaHSFA4a (Fig. 2A). Multiple alignment results revealed that PuHSFA4a shares ~40% to 56% of its amino acid sequence identity with homologous proteins in other plants species (Fig. 2B). Structure analysis showed that PuHSFA4a is a typical class A HSF and contains motifs typical of that class of proteins, including a predicted nuclear localization signal (NLS) domain and a nuclear export signal (NES) that is responsible for nuclear and cytoplasmic localization (Lyck et al., 1997; Li et al., 2018). However, the conserved DNA-binding domain (DBD) of PuHSFA4a does not contain the amino acids

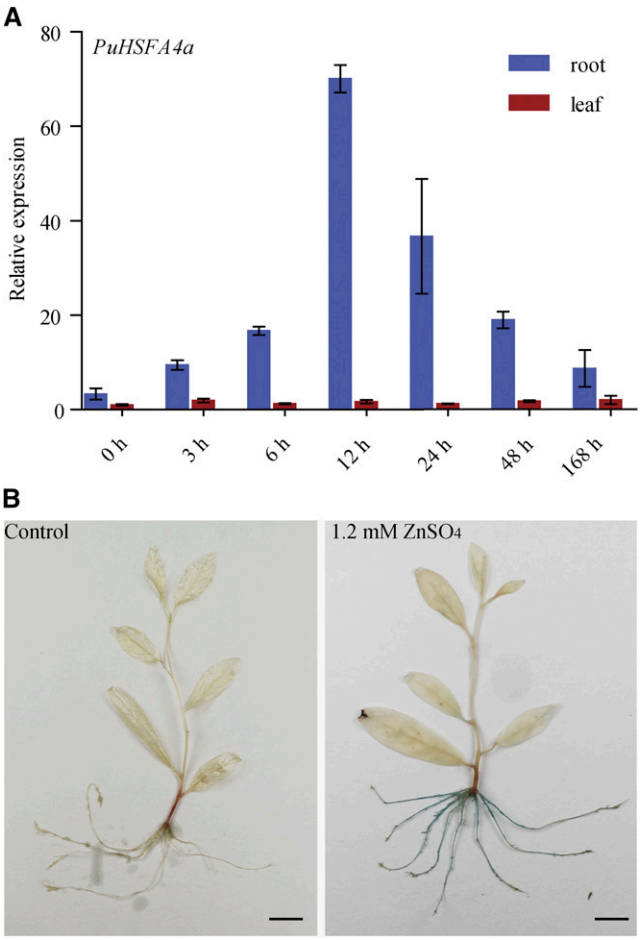

Figure 1. Relative expression of *PuHSFA4a* in roots and leaves of *P. ussuriensis* and histochemical analysis of the expression of the *PuHSFA4a* promoter in *P. ussuriensis* tissues as visualized by glucuronidase staining under excess Zn. A, Relative expression of *PuHSFA4a* in roots and leaves under excess Zn. Two-week–old plants were grown in media supplemented with 1.2 mM of $ZnSO_4$ for 0–48 h and 1 week. Data are presented as means of three biological replicates, and error bars = SD. B, GUS activity staining of ProPuHSFA4a::*GUS* transgenic plants that were grown on half strength Murashige and Skoog (MS) medium supplemented with or without 1.2 mM of $ZnSO_4$ for 1 week. Scale bars = 1 cm.

Ala-31 and Leu-42, two changes linked to Cd tolerance in TaHSFA4a (Shim et al., 2009).

PuHSFA4a Is Localized in the Nucleus and the Cytoplasm and Functions as a Transcriptional Activator

We generated a 35S::*PuHSFA4a-GFP* plasmid by inserting a GFP tag at the 3′end of the *PuHSFA4a* gene. The fusion genes 35S::*PuHSFA4a-GFP* and 35S::*GFP* were transiently transformed into *P. ussuriensis* leaves, after which we performed an immunoblot analysis using an anti-GFP antibody (Supplemental Fig. S2). The results of this experiment revealed two bands distinguishing the PuHSFA4a-GFP and GFP proteins, thereby confirming that PuHSFA4a-GFP was a fusion protein (Supplemental Fig. S2). Subcellular localization of the PuHSFA4a protein was examined by expressing a GFP fusion construct that was introduced into onion (*Allium cepa*) epidermal cells. The results showed that the control (i.e. construct only containing GFP) was distributed throughout the cell. In contrast, the *PuHSFA4a-GFP* fusion protein was observed only in the nucleus and the cytoplasm (Fig. 3A). These results are similar to LlHSFA1, which is localized primarily in the nucleus, but is also present in the cytoplasm (Gong et al., 2014). PuHSFA4a has six domains. These include an N-terminal DBD, a hydrophobic heptad repeat region for oligomerization, a nuclear import signal (NLS), a Leu-rich NES, and the transcriptional activator domains activator of Hsp90 ATPase 1 (AHA1) and AHA2. Correspondingly, we divided PuHSFA4a into six parts, with each part containing a structural domain (Fig. 3B). To measure the transactivation activity of PuHSFA4a, various versions of PuHSFA4a (Fig. 3B) were constructed and inserted into pGBKT7 vectors before transformation into AH109 yeast strains. The transactivation activity of PuHSFA4a was examined by assessing yeast transformant growth on a selection medium (SD/-Trp-His-Ade) or determined by assessing β-galactosidase (β-gal) activity. Expression of the PuHSFA4a full-length fusion protein in yeast resulted in high expression of the reporter gene, demonstrating that PuHSFA4a had strong activity as a transcription activator. Deletion of the region between amino acids 214 and 278 decreased the transactivation activity of PuHSFA4a, while deletion of other domains did not alter this activity. β-gal activity assays further confirmed these results. Taken together, these findings reveal both that PuHSFA4a acts as a transcriptional activator and that the region between amino acids 214 and 278—which contains the AHA1 domain—was required for transcription activation (Fig. 3B).

PuHSFA4a Positively Regulates Root Growth under Excess Zn in *P. ussuriensis*

To investigate the function of *PuHSFA4a*, we generated overexpression *PuHSFA4a* transgenic lines of *P. ussuriensis* (*PuHSFA4a*-OE). We also generated *PuHSFA4a* dominant repressor lines (*PuHSFA4a-SRDX*) of *P. ussuriensis* using Chimeric Repressor Silencing Technology by fusing the full-length *PuHSFA4a* gene in frame with the *SRDX* repression domain (for SUPERMAN repression domain; Chai et al., 2014). The elevated expression of *PuHSFA4a* was confirmed in independent *PuHSFA4a*-OE lines and the elevated expression of *PuHSFA4a-SRDX* fusion gene was confirmed in independent *PuHSFA4a-SRDX* lines by RT-qPCR (Supplemental Fig. S3, A and B). Under normal conditions, both *PuHSFA4a*-OE and *PuHSFA4a-SRDX* transgenic plants showed the same phenotype relative to the wild type (Fig. 4; Supplemental Fig. S3C). After exposure to high Zn stress, the *PuHSFA4a*-OE lines had higher root dry weight and plant height than wild-type plants (Fig. 4, A–C; Supplemental Fig. S3C), while

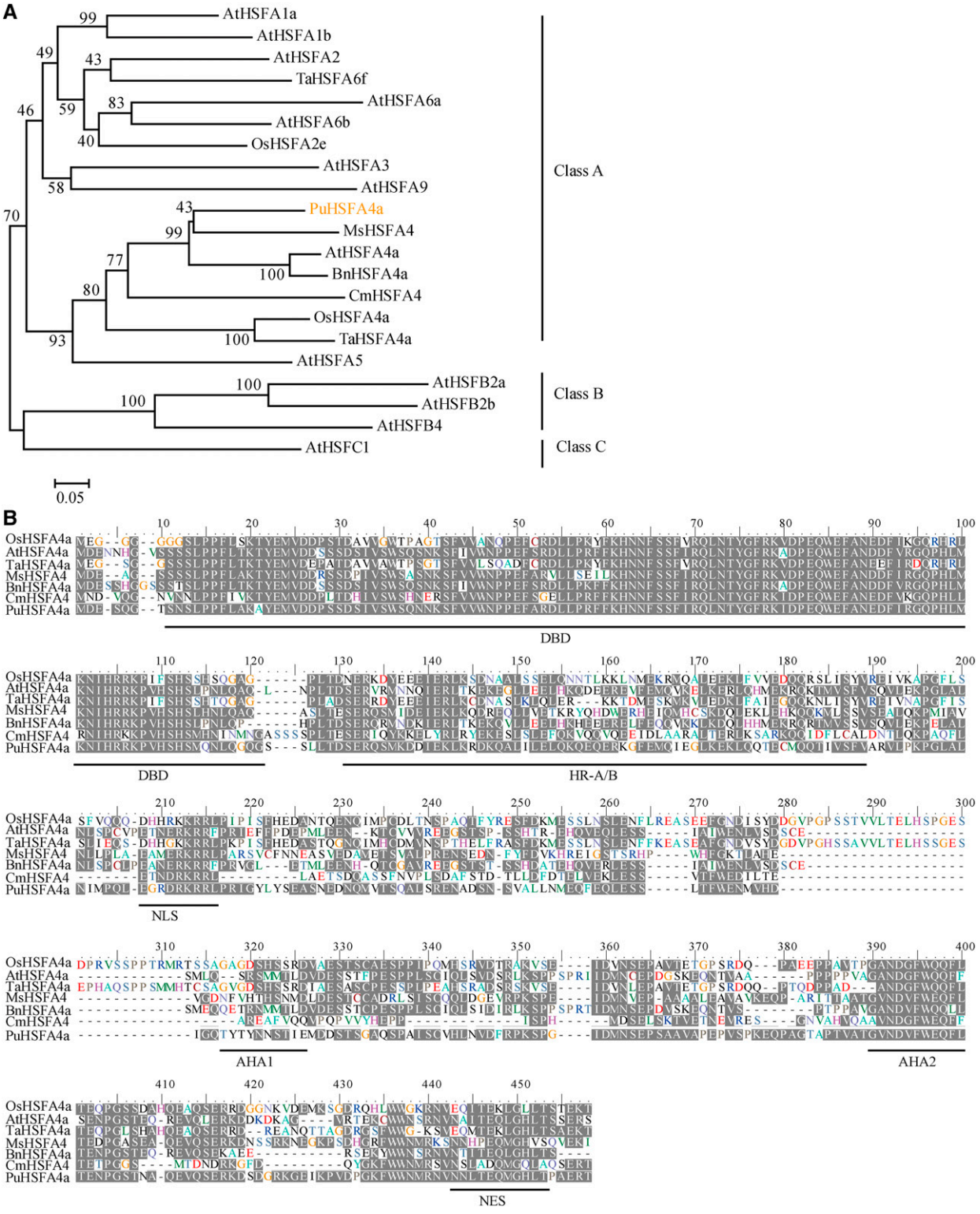

Figure 2. Phylogenetic tree and multiple sequence alignments of HSF proteins. A, Phylogenetic tree of HSF proteins. The number next to the branches is the percentage of trees that relate to taxa clustered together. B, Multiple sequence alignment of the HSFA4a amino acid sequence in *P. ussuriensis* (PuHSFA4a), Arabidopsis (AtHSFA4a), *Triticum aestivum* (TaHSFA4a), rice (OsHSFA4a), *B. napus* (BnHSFA4a), *Medicago sativa* (MsHSFA4a), and *Chrysanthemum* (CmHSFA4a). PuHSFA4a contains six domains: the DBD, the hydrophobic heptad repeat region for oligomerization (HR-A/B), the NLS, the transcriptional activators AHA1 and AHA2, and the Leu-rich NES domains (underlined in black).

PuHSFA4a-SRDX lines displayed significantly inhibited root growth (Fig. 4, A–C).

After two months of growth in normal soil followed by four weeks of growth while being irrigated with 5 mM of $ZnSO_4$ solution (Fig. 5A), the root dry weight, plant height, and chlorophyll content of leaves from *PuHSFA4a*-OE line plants were all significantly higher than those of wild-type plants (Fig. 5, A–D). In contrast, the root dry weight and chlorophyll content of *PuHSFA4a-SRDX* plants were significantly lower than in wild-type plants (Fig. 5, A–D). The root Zn concentration was significantly higher in *PuHSFA4a*-OE lines and lower in *PuHSFA4a-SRDX* lines relative to wild-type roots when irrigated with 5 mM of $ZnSO_4$ solution (Fig. 5E). By contrast, after two weeks, aboveground and root growth were similar in *PuHSFA4a*-OE, *PuHSFA4a-SRDX*, and wild-type plants exposed to high Cu, Fe, Cd, ABA, NaCl, and PEG6000 stress (Supplemental Fig. S4).

PuHSFA4a Overexpression Decreased ROS Production in Roots under Excess Zn

Electrolyte leakage (EL) and malondialdehyde (MDA) are two widely used indicators of damage caused by abiotic stress. Under normal growth conditions, EL and MDA content was similar in transgenic lines and wild-type roots. However, under excess Zn, *PuHSFA4a*-OE lines showed decreases of ~37% in EL and ~35% in MDA content in roots compared to wild-type plants (Fig. 4D; Supplemental Fig. S3D). In addition, *PuHSFA4a-SRDX* plants displayed a higher EL and MDA than the wild type in roots (Fig. 4D; Supplemental Fig. S3D). Next, hydrogen peroxide (H_2O_2) levels were compared in roots among *PuHSFA4a*-OE, *PuHSFA4a-SRDX*, and wild-type plants under excess Zn (Fig. 4, E and F). No visible differences in H_2O_2 levels were detected between transgenic lines and wild-type roots under control conditions. In the presence of excess Zn, *PuHSFA4a*-OE lines were stained lighter compared with wild type, while *PuHSFA4a-SRDX* lines were stained darker than wild type (Fig. 4E). These results were further confirmed using quantitative measurements (Fig. 4F), implying that the roots of *PuHSFA4a*-OE plants had significantly less H_2O_2 content compared with wild-type plants, whereas *PuHSFA4a-SRDX* plants had significantly higher H_2O_2 content than wild-type plants (Fig. 4, E and F).

PuHSFA4a Regulates Genes Involved in Abiotic Stress Responses and Root Development

To identify genes regulated by PuHSFA4a in response to Zn-induced stress in roots, we performed RNA sequencing (RNA-seq) experiments using *PuHSFA4a*-OE and wild-type plant roots that were either treated with 1.2 mM of $ZnSO_4$ for two weeks or were mock-treated as a control. We found 733 upregulated and 708 downregulated genes when comparing control and excess Zn-stressed wild-type plants (false discovery rate [FDR]-adjusted P value < 0.01), and 485 upregulated and 479 downregulated genes when making the same comparison of *PuHSFA4a*-OE plants (FDR-adjusted P value < 0.01; Supplemental Tables S1 and S2). Pairwise comparisons of relative expression data revealed that 33 genes showed substantially differences in expression between *PuHSFA4a*-OE and wild-type plants including three common genes (FDR-adjusted P value < 0.01). These genes included 17 genes under normal conditions and 19 genes under excess Zn treatment (Fig. 6A; Supplemental Tables S3 and S4). Gene Ontology term enrichment analysis was performed on the 33 differentially expressed genes (DEGs) between *PuHSFA4a*-OE and wild-type roots. Our results showed enrichment of genes in pathways related to: cellular responses to hypoxia, monocarboxylic acid biosynthetic processes, and lateral root formation. In general, these pathways are involved in defense and root growth (Supplemental Fig. S5). We found that overexpressing *PuHSFA4a* resulted in the upregulation of 16 abiotic stress-related genes. We validated our RNA-seq results via RT-qPCR analysis. The results of this validation for the expression levels of these 16 upregulated stress-response DEGs are shown in Figure 6B. All selected genes showed similar expression patterns in our RT-qPCR and RNA-seq analyses (Supplemental Tables S3 and S4).

PuHSFA4 Binds To the Promoter Regions of *PuGSTU17* and $PuPLA_2$

We used the PlantCARE and Plant PAN databases to search for putative heat shock elements (HSEs) in the ~2-kb promoter regions of each of the 16 selected genes that were upregulated in *PuHSFA4a*-OE plants. From these searches, we found 13 genes that contained enriched HSE elements in their promoter regions (primers shown in Supplemental Table S5). Chromatin immunoprecipitation (ChIP)-PCR assays with anti-GFP from 35S::*PuHSFA4a-GFP* plants were used to test the capacity of PuHSFA4a to bind to the promoters of these 13 predicted target genes. ChIP-PCR showed robust enrichment of *PuHSFA4a-GFP* in the promoter regions of *PuGSTU17* and $PuPLA_2$, but not in the promoters of the other 11 genes (Supplemental Fig. S6). Another ChIP-qPCR analysis with anti-GFP antibody verified that the *PuGSTU17* and $PuPLA_2$ promoters showed significantly higher PuHSFA4a binding enrichment at binding sites relative to a control (Fig. 7A). Yeast one-hybrid (Y1H) assays showed that when fused *PuGSTU17*-AbAi or $PuPLA_2$-AbAi was coexpressed with *PuHSFA4a*-AD in yeast, the two strains could grow on SD/-Ura/-Leu/AbA plates (Fig. 7B). This result revealed that PuHSFA4a bound specifically to the promoters of the *PuGSTU17* and $PuPLA_2$ genes in vivo. A luciferase reporter (LUC) assay showed that coexpression of 35S::*PuHSFA4a* with ProPuGSTU17::*Luc* or

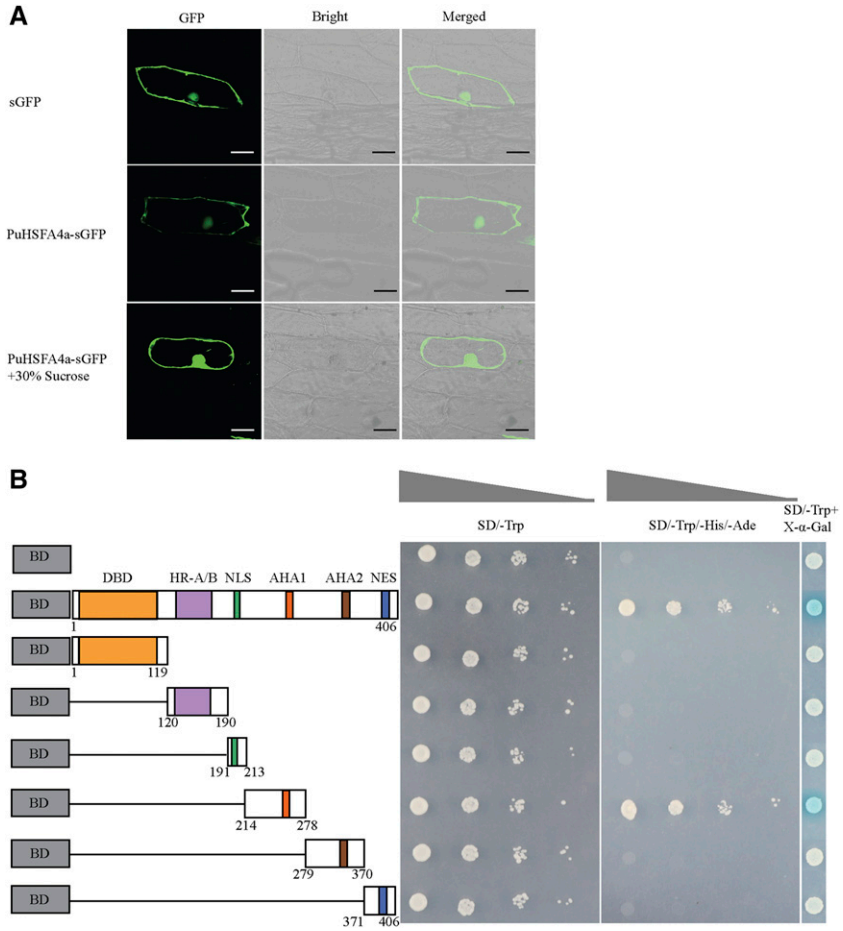

Figure 3. Subcellular localization and transactivation assay of PuHSFA4a. A, Subcellular localization of GFP fusion PuHSFA4a protein in onion epidermal cells. Images were obtained in a dark field to detect green fluorescence, and again in bright light to observe the morphological characteristics of the cells. Bars = 50 μm. B, Transactivation assay of PuHSFA4a in yeast cells. The full-length construct and several partial deletion constructs of *PuHSFA4a* were fused to GAL4 DBD and expressed in the yeast strain AH109 Gold. Transformed yeast was grown in either SD/-Trp or SD/-Trp/-His/-Ade media. pGBKT7 was used as a negative control. LacZ activity was observed in SD/-Trp medium containing X-α-Gal.

ProPuPLA$_2$::*Luc* led to an obvious increase in luminescence intensity (Fig. 7C), thus confirming that PuHSFA4a interacts with the promoters of *PuGSTU17* and *PuPLA$_2$*. Additionally, an electrophoretic mobility shift assay (EMSA) showed that PuHSFA4a bound to a DNA probe containing a typical HSE motif (GAACTTTC or TTCAAGAA) was out-competed by an unlabeled DNA probe. In contrast, PuHSFA4a failed to bind to a mutant probe (Fig. 7D). A further RT-qPCR experiment showed that the expression of *PuGSTU17* was significantly reduced under Zn stress in the roots of *PuHSFA4a-SRDX* lines relative to wild-type plants (Fig. 7E). Taken together, these results demonstrate that PuHSFA4a positively regulates *PuGSTU17* and *PuPLA$_2$* expression in response to high Zn stress by binding directly to their promoter regions.

PuGSTU17 Positively Regulates Zn Tolerance and ROS Scavenging Capacity in Roots

To determine whether *PuGSTU17* confers Zn tolerance, we generated 35S::*PuGSTU17* (*PuGSTU17*-OE) lines of *P. ussuriensis*, and also generated *PuGSTU17*-RNA interference (RNAi) lines of *P. ussuriensis* (*PuGSTU17*-RNAi). The expression of *PuGSTU17* was confirmed in transgenic lines by RT-qPCR (Supplemental Fig. S7). Under normal culture conditions, *PuGSTU17*-OE and *PuGSTU17*-RNAi plants showed the same phenotype as wild-type plants (Supplemental Fig. S7). When plants were cultured on media containing 1.2 mM of $ZnSO_4$ for two weeks, plant heights were not significantly different between *PuGSTU17* transgenic lines and wild-type plants. However, the root dry weight of *PuGSTU17*-OE plants was significantly higher than that of wild-type plants, while *PuGSTU17*-RNAi lines displayed significantly inhibited root growth (Fig. 8, A and B). Moreover, *PuGSTU17*-OE plant roots had lowered EL and MDA content than wild-type plants when exposed to high Zn stress while *PuGSTU17*-RNAi plants displayed a higher EL and MDA than the wild type in roots (Fig. 8, C and D). Our results showed that *PuGSTU17*-OE plants suffered less cell membrane damage than wild-type and *PuGSTU17*-RNAi plants. In addition, quantitated H_2O_2 content data indicated that roots of *PuGSTU17*-OE plants displayed lower, and *PuGSTU17*-RNAi plants had higher, ROS levels than wild type under Zn stress (Fig. 8E).

We quantified the GST activity of roots of *PuGSTU17*-OE, *PuGSTU17*-RNAi, and wild-type plants. Under excess Zn stress, the GST activity of the roots of *PuGSTU17*-OE plants was higher than the activity of the roots of

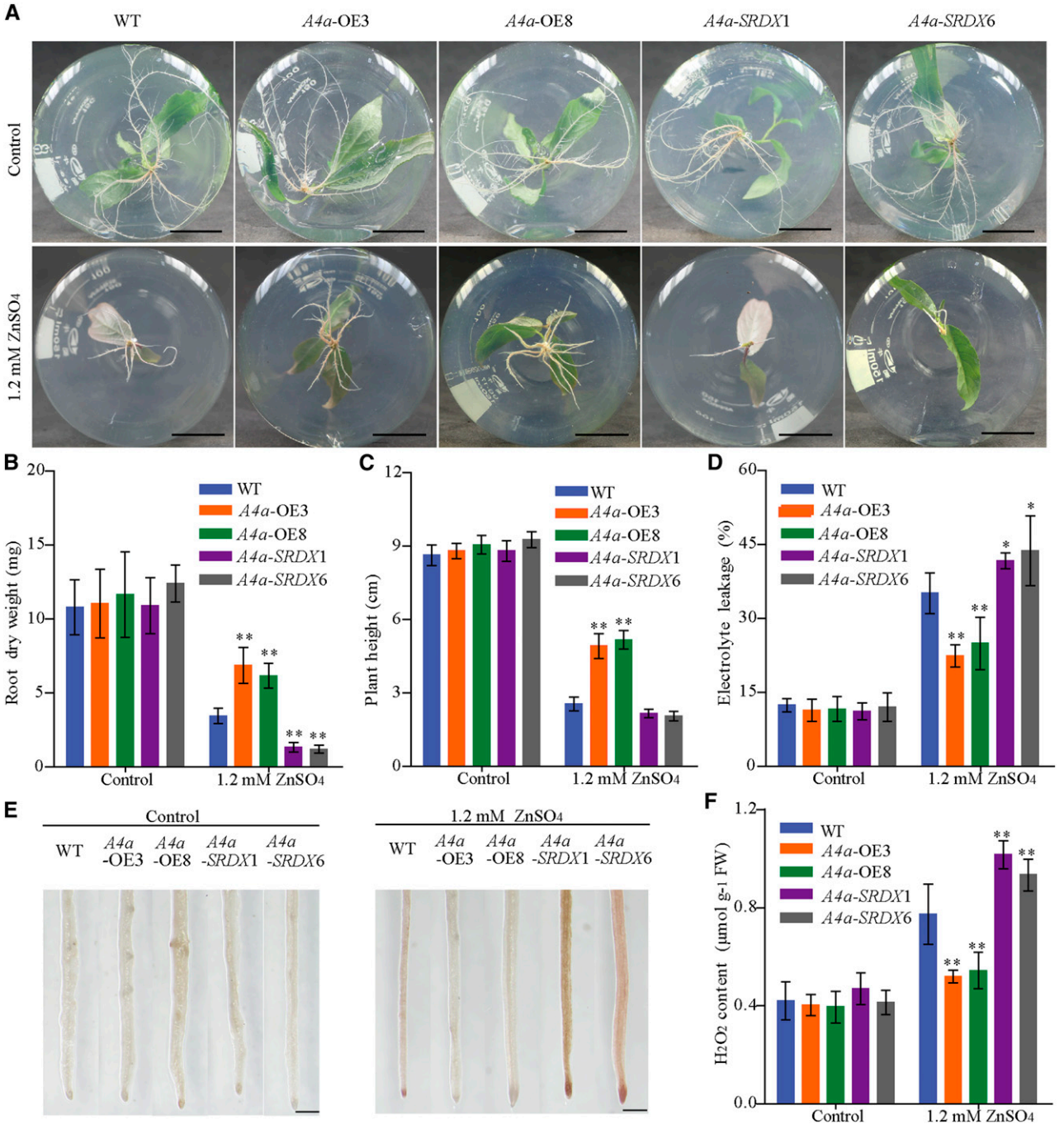

Figure 4. Phenotypes of wild-type, *PuHSFA4a*-overexpression (*A4a*-OE3 and *A4a*-OE8), and *PuHSFA4a-SRDX* dominant repressor (*A4a-SRDX*1 and *A4a-SRDX*6) *P. ussuriensis* plants. A, Phenotypes of *A4a*-OE3, *A4a*-OE8, *A4a-SRDX*1, *A4a-SRDX*6, and wild-type (WT) plant roots grown with or without 1.2 mM of $ZnSO_4$ for two weeks. Scale bars = 2 cm. B and C, Root dry weight (B) and plant height (C) of *A4a*-OE3, *A4a*-OE8, *A4a-SRDX*1, *A4a-SRDX*6, and wild-type plants with or without 1.2 mM of $ZnSO_4$. Each value represents the mean of 30 plants, and error bars = SD. D, Measurement of EL in *A4a*-OE3, *A4a*-OE8, *A4a-SRDX*1, *A4a-SRDX*6, and wild-type plants with or without 1.2 mM of $ZnSO_4$. Data are presented as means of six biological replicates, and error bars = SD. E and F, In situ accumulation of H_2O_2 in wild-type and transgenic plants, as revealed by histochemical staining with DAB with or without 1.2 mM of $ZnSO_4$ (E). Scale bars = 500 μm. Measurement of the H_2O_2 content of roots in wild-type and transgenic plants by luminol assay as described in the "Materials and Methods" (F). Data are presented as means of three biological replicates, and error bars = SD. In (B), (C), (D), and (F), Asterisks indicate significant differences as determined by a Student's *t* test, $*P < 0.05$ and $**P < 0.01$.

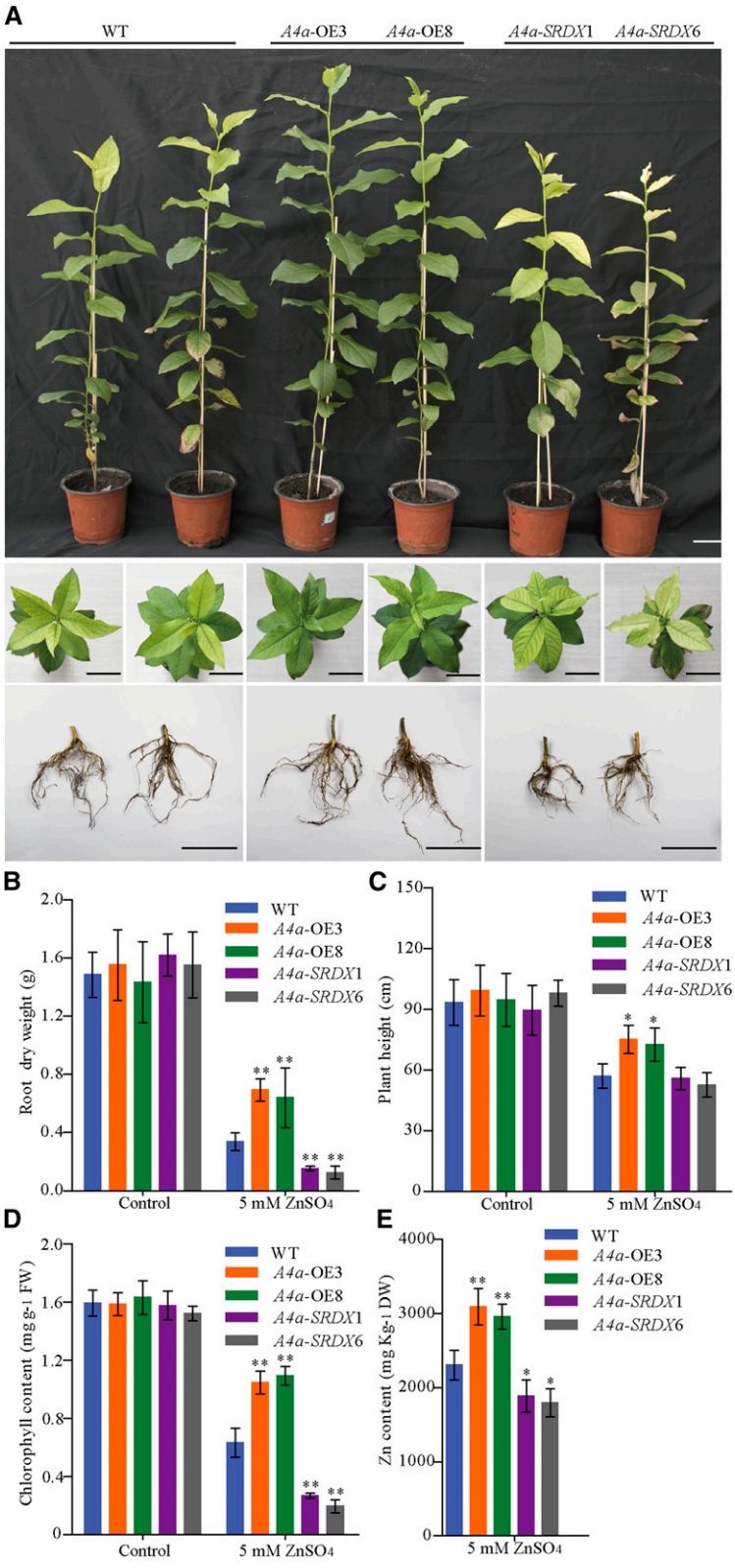

Figure 5. Phenotypes of *PuHSFA4a*-OE, *PuHSFA4a-SRDX* dominant repressor, and wild-type (WT) *P. ussuriensis* plants after transplantation in soil under excess Zn. A, Phenotypic comparison of *PuHSFA4a* transgenic and wild-type plants with respect to above-ground parts, leaves, and roots after irrigation with 5.0 mM of $ZnSO_4$ for four weeks. Scale bars = 5 cm. B and C, Root dry weight (B) and plant height (C) of *A4a*-OE3, *A4a*-OE8, *A4a-SRDX*1, *A4a-SRDX*6, and wild-type *P. ussuriensis* plants in response to excess Zn. Each value represents the mean of 40 plants, and error bars = SD. D, Chlorophyll content of leaves of *PuHSFA4a* transgenic and wild-type plants with or without excess Zn treatment. E, Zn content of *PuHSFA4a* transgenic and wild-type plants roots under excess Zn treatment. Two-month–old plants were treated with 5.0 mM of $ZnSO_4$ for four weeks. Data are presented as means of three biological replicates, and error bars = SD. Asterisks indicate significant differences as determined by a Student's *t* test, $*P < 0.05$ and $**P < 0.01$.

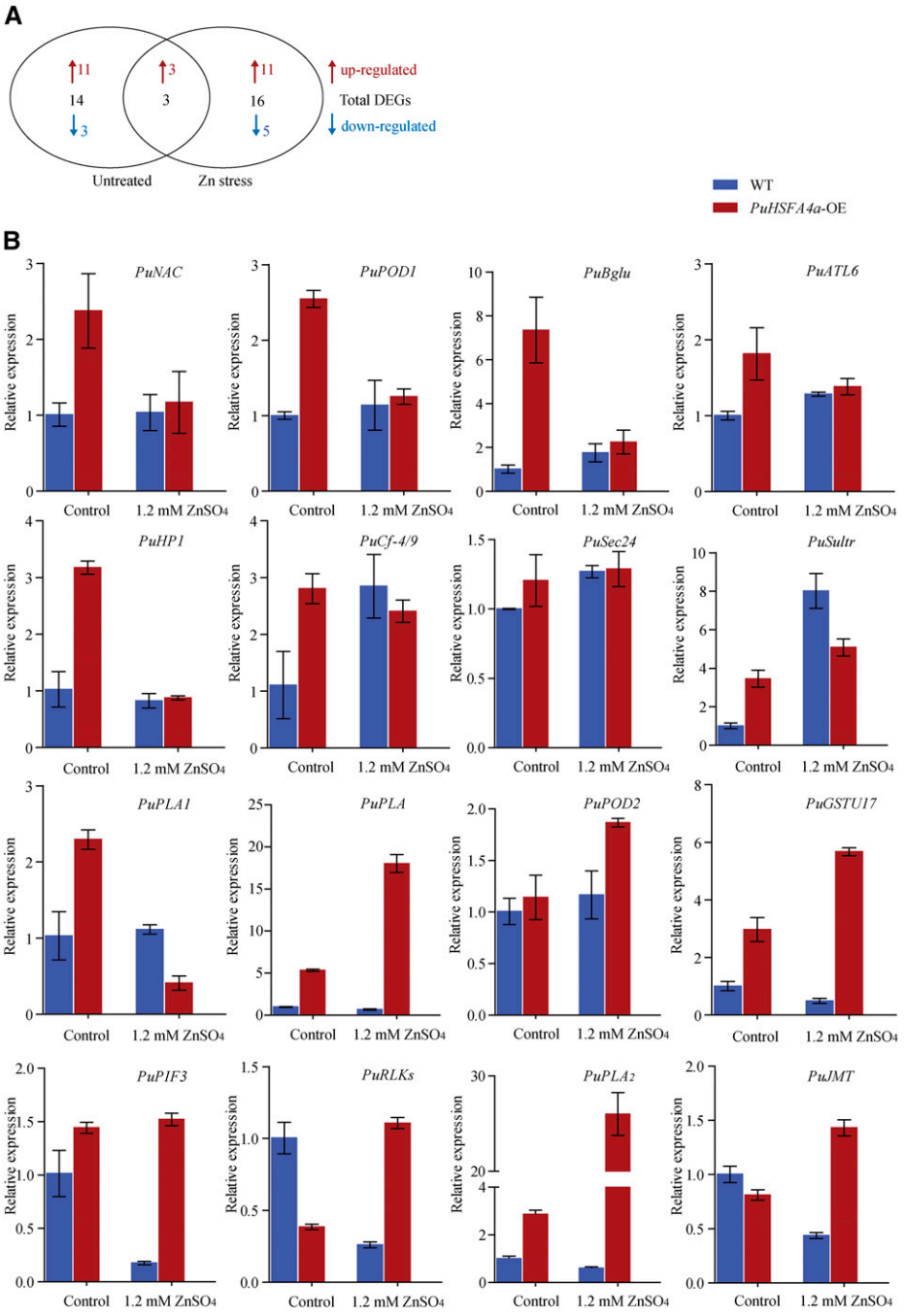

Figure 6. Transcriptome analyses of *PuHSFA4a* overexpression and wild-type (WT) *P. ussuriensis* plants under high Zn stress. A, Venn diagrams comparing the DEGs among the *PuHSFA4a*-OE and wild-type *P. ussuriensis* lines with or without 1.2 mM of $ZnSO_4$. "Untreated" represents the DEGs between wild-type and *PuHSFA4a*-OE under control conditions. "Zn stress" represents the DEGs between wild-type and *PuHSFA4a*-OE under high Zn stress. Red and blue colors indicate upregulated and downregulated genes, respectively. B, RT-qPCR analysis of the transcript levels of *PuHSFA4a* target genes with or without 1.2 mM of $ZnSO_4$. Data are presented as means of three biological replicates, and error bars = SD.

wild-type plants (Fig. 8F). After inhibiting the expression of *PuGSTU17*, the GST activity in roots was lower compared with wild type (Fig. 8F). In addition, we assessed GST activity in the roots of *PuHSFA4a*-OE, *PuHSFA4a-SRDX*, and wild-type plants. The results showed *PuHSFA4a*-OE lines displayed significantly higher, and *PuHSFA4a-SRDX* lines had lower, root GST activity than wild type under high Zn stress (Fig. 8G). The root Zn concentration was higher in *PuGSTU17*-OE lines and lower in *PuGSTU17*-RNAi lines relative to wild-type roots when irrigated with a 1.2-mM $ZnSO_4$ solution (Supplemental Fig. S7D). Next, we compared plant tolerance to $CdCl_2$, PEG6000, and NaCl stresses in *PuGSTU17*-OE and wild-type plants. These comparisons revealed no phenotypic differences between *PuGSTU17*-OE and wild-type plants in response to these stresses for 2 weeks (Supplemental Fig. S8, A–D).

PuPLA$_2$ Overexpression Increased Root Growth under Excess Zn

We then used the plant expression vector 35S::*PuPLA*$_2$ to overexpress *PuPLA*$_2$ (*PuPLA*$_2$-OE) in

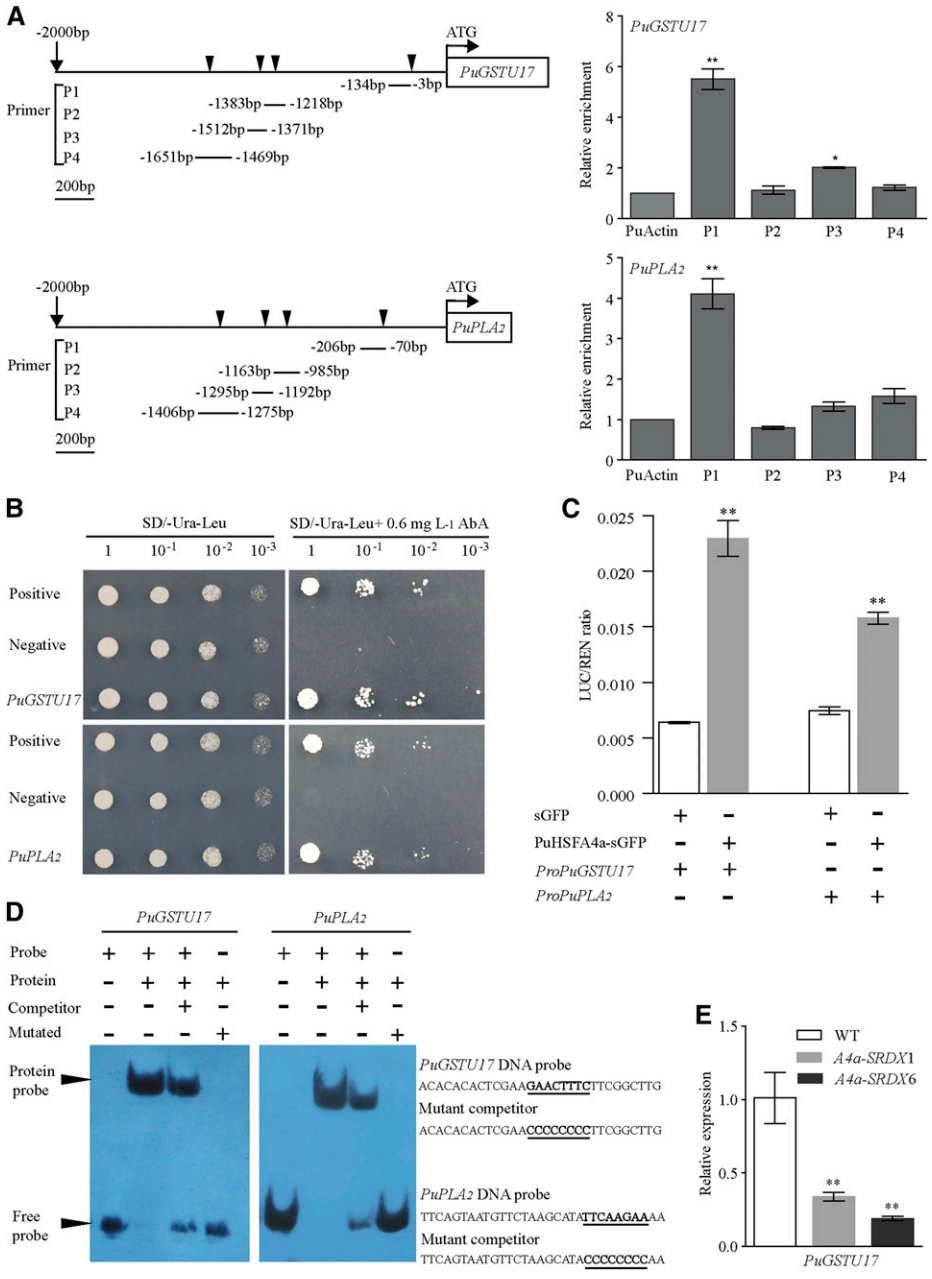

Figure 7. Verification of the PuHSFA4a target genes *PuGSTU17* and *PuPLA*$_2$. A, ChIP-qPCR analysis of PuHSFA4a binding to *PuGSTU17* and *PuPLA2* promoter fragments using anti-GFP tag antibody. Schematic diagrams showing the PuHSFA4a binding sites in the regions 2,000 bp upstream of the transcriptional start (ATG) sites of the *PuGSTU17* and *PuPLA*$_2$ genes. Triangular arrowheads indicate PuHSFA4a binding sites (P1, P2, P3, and P4). B, Y1H assay of PuHSFA4a binding to *PuGSTU17* and *PuPLA*$_2$ promoter fragments. C, Binding of PuHSFA4a to the promoters of *PuGSTU17* and *PuPLA*$_2$ as assayed using the dual luciferase system. D, EMSA analyses showing the binding of PuHSFA4a to the DNA probes of the *PuGSTU17* and *PuPLA*$_2$ promoters in vitro. The free and bound DNAs (arrows) were separated by acrylamide gel electrophoresis. The unlabeled probes were used as competitors, and mutated probes were produced by replacing the HSE motifs with GGGGGGGG. E, Relative expression levels of *PuGSTU17* in *PuHSFA4a-SRDX* and wild-type plants assessed under excess Zn conditions and normalized to *PuActin* (MH644084). In (A), (C), and (E), data are presented as means of three biological replicates, and error bars = SD. Asterisks indicate significant differences as determined by a Student's *t* test, $*P < 0.05$ and $**P < 0.01$.

P. ussuriensis. The expression levels of *PuPLA*$_2$ were significantly increased in *PuPLA*$_2$ overexpression (*PLA*$_2$-OE2, *PLA*$_2$-OE3) lines than in wild-type plants (Supplemental Fig. S9A). Under normal culture conditions in vitro, *PuPLA*$_2$-OE plants had larger root systems than wild-type plants (Fig. 9, A and B). In contrast, plant height did not significantly differ between *PuPLA*$_2$-OE and wild-type plants (Fig. 9C). When cultured on media containing 1.2 mM of $ZnSO_4$ for 2 weeks, root growth and plant height of both transgenic and wild-type plants were suppressed. However, under high Zn stress, *PuPLA*$_2$-OE lines showed higher root dry weight and plant height than wild-type plants (Fig. 9, A–C; Supplemental Fig. S9B). To further determine the role played by PuPLA$_2$ in the Zn stress response, we assessed the expression of the auxin signaling-related gene *Phytochrome-Interacting Factor 3* (*PuPIF3*), which was upregulated in *PuHSFA4a*-OE plants under Zn stress (Supplemental Table S4). We then found that, in response to excess Zn, *PuPIF3* showed increased expression in *PuPLA*$_2$-OE lines relative to wild-type plants (Fig. 9D).

DISCUSSION

Plant HSFs are known to be involved in abiotic stress responses, including to heat, salt, oxidative, drought, Cd, and starvation stresses (Panchuk et al., 2002; von Koskull-Döring et al., 2007; Shim et al., 2009; Pérez-Salamó et al.,

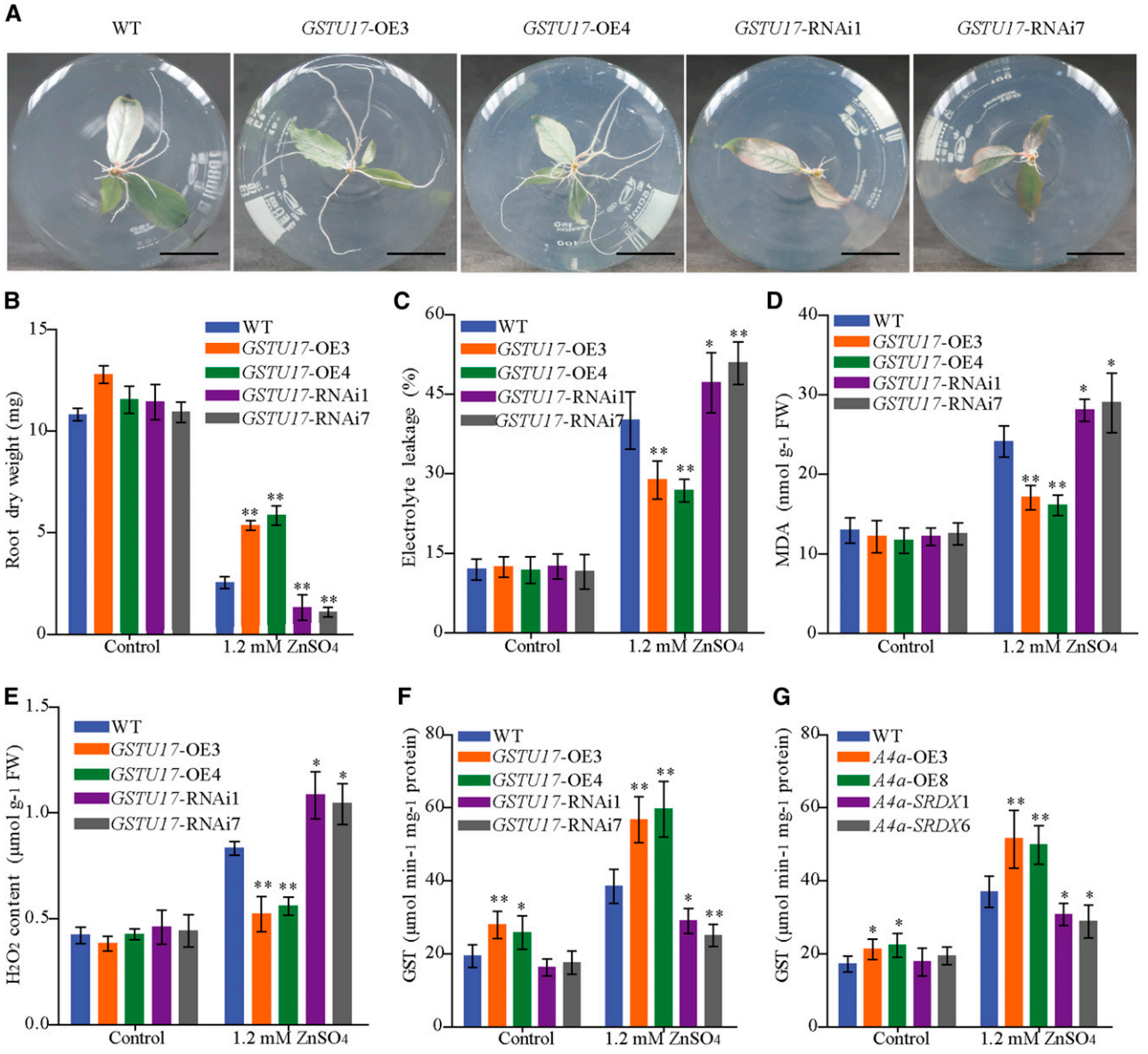

Figure 8. Phenotype of *PuGSTU17*-overexpression (*GSTU17*-OE3 and *GSTU17*-OE4), *PuGSTU17*-RNAi (*GSTU17*-RNAi1 and *GSTU17*-RNAi7), and wild-type (WT) *P. ussuriensis* plants under excess Zn. A, Phenotypic comparison of the roots of *PuGSTU17*-OE, *PuGSTU17*-RNAi, and wild-type plants in response to excess Zn. Scale bars = 2 cm. B, Root dry weight of *PuGSTU17*-OE, *PuGSTU17*-RNAi, and wild-type plants with or without Zn treatment. Each value represents the mean of 30 plants, and error bars = SD. C, Measurement of EL in *PuGSTU17*-OE, *PuGSTU17*-RNAi, and wild-type plants with or without Zn treatment. D, Measurement of MDA in *PuGSTU17*-OE, *PuGSTU17*-RNAi, and wild-type plants with or without Zn treatment. E, Measurement of the H_2O_2 content in *PuGSTU17*-OE, *PuGSTU17*-RNAi, and wild-type plants with or without Zn treatment. F, Measurement of GST activity in *PuGSTU17*-OE, *PuGSTU17*-RNAi, and wild-type plants with or without Zn treatment. G, Measurement of GST activity in *PuHSFA4a*-OE, *PuHSFA4a-SRDX*, and wild-type plants with or without Zn treatment. In (C) to (G), data are presented as means of three biological replicates, and error bars = SD. Asterisks indicate significant differences as determined by a Student's *t* test, $*P < 0.05$ and $**P < 0.01$.

2014). However, to date there are no reports of plant HSFs that are specifically involved in the Zn stress response. In this study, we characterized PuHSFA4a, an HSF found in *P. ussuriensis* that acts as a positive regulator of excess Zn tolerance in roots. *PuHSFA4a* is specifically induced in root tissues by excess Zn. When exposed to excess Zn, a dominant repressor version of the *PuHSFA4a* lines (*PuHSFA4a-SRDX*) decreased Zn tolerance and root growth, while *PuHSFA4a* overexpression (*PuHSFA4a*-OE) significantly increased Zn tolerance and root growth. Moreover, we also found that PuHSFA4a contributed to excess Zn tolerance by directly regulating *PuGSTU17* to control ROS levels in roots. *PuHSFA4a* overexpression was also found to enhance Zn tolerance by largely

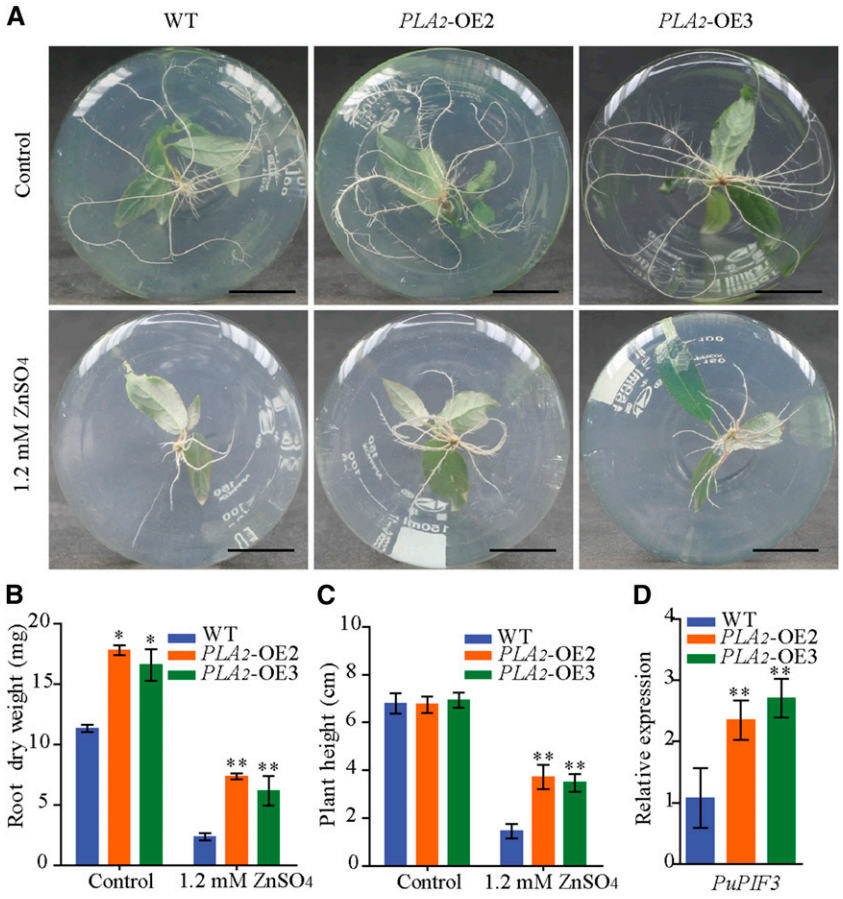

Figure 9. Phenotype of *PuPLA$_2$*-OE and wild-type (WT) *P. ussuriensis* plants with or without Zn treatment. A, Phenotypic comparison of the roots of *PuPLA$_2$* transgenic and wild-type plants with or without excess Zn. Scale bars = 2 cm. B and C, Root dry weight (B) and plant height (C) of *PuPLA$_2$*-OE and wild-type plants under excess Zn stress. Each value represents the mean of 30 plants, and error bars = SD. D, The relative expression levels of *PuPIF3* in *PuPLA$_2$*-OE and wild-type plants assessed under excess Zn conditions, and a comparison of the relative expression of *PuPIF3* in *PuPLA$_2$*-OE lines compared to wild-type plants. All values are normalized to *PuActin* (MH644084). Data are presented as means of three biological replicates, and error bars = SD. For (B)–(D), Asterisks indicate significant differences as determined by a Student's *t* test, $*P < 0.05$ and $**P < 0.01$.

upregulating target *PuPLA$_2$* transcript levels, and thus promoting root growth when exposed to high levels of Zn. These results demonstrate that PuHSFA4a functions positively in regulating excess Zn response.

Because roots are the first tissue confronted by excess heavy metal content in the soil, toxic symptoms of excess exposure to heavy metals are more common in roots than in other tissues (Chang et al., 2005). The primary response to Zn toxicity is growth inhibition, often characterized by reduced root growth, increased root thickening, and impaired cell division/elongation (Barceló and Poschenrieder, 1990; Vaillant et al., 2005). For instance, overexpression of the *ACS* gene in Arabidopsis improves tolerance to excess Fe by protecting growing roots (Li et al., 2015). Moreover, in response to stress caused by exposure to excess Cd, suppression of *GPL4* in Arabidopsis results in increased root biomass and tolerance to Cd (Khare et al., 2017). Overexpression of *MAN3* in Arabidopsis in response to excess Cd also results in larger roots (i.e. roots with heavier root fresh weights) and enhanced Cd tolerance (Chen et al., 2015). In this study, under excess Zn, *PuHSFA4a*-OE transgenic line plants showed lower root ROS, MDA, and EL levels and stronger root systems than wild-type plants, whereas *PuHSFA4a-SRDX* plants had higher root ROS, MDA, and EL levels and weaker roots than wild-type plants. Previous studies have reported mechanisms by which plants have evolved to cope with excess ROS induced by Zn stress, mainly by activating antioxidant enzymes and by producing nonenzymatic compounds (Chaoui et al., 1997; Wang et al., 2009). For example, overexpression of *HvAPX1* in barley alleviated Zn toxicity-induced damage in Arabidopsis by limiting oxidative damage (Xu et al., 2008). Based on these findings, we speculate that *PuHSFA4* confers tolerance to excess Zn by regulating ROS levels and membrane lipid peroxidation to ensure root cell integrity.

Transcriptomic analysis of *PuHSFA4a*-OE and wild-type *Populus* roots identified many genes whose expression was substantially regulated by *PuHSFA4a* overexpression. Consistent with the observed phenotype changes, expression of genes related to abiotic stress response and root growth were increased substantially by high Zn stress in roots. In the last decade, many studies have improved our understanding of the molecular mechanisms that regulate excess Zn tolerance. For example, *MTP1* from *P. trichocarpa* × *P. deltoides* (Blaudez et al., 2003), *AtHMA1* (Kim et al., 2009), *AtHMA3* (Morel et al., 2009), *AtMTP1* (Desbrosses-Fonrouge et al., 2005), *AtMTP3* (Arrivault et al., 2006), *AQUA1* (Ariani et al., 2016), *OZT1* (Lan et al., 2013), the cyanobacterial metallothionein gene *SmtA* (Xu et al., 2010), and *HvAPX1* (Xu et al., 2008) have all been found to contribute to the detoxification of excess Zn in diverse species. In this study, transcriptomic analysis revealed that overexpression of *PuHSFA4a* did not affect

the expression of any previously identified Zn stress response genes. In addition, studies of various other plant species have identified target genes regulated by HSFA4as, including the *Arabidopsis HSP17.6A* (Pérez-Salamó et al., 2014) and yeast *MT* (Shim et al., 2009) genes. However, our RNA-seq data did not reveal any known target genes that were affected by *PuHSFA4a* expression. Collectively, our results suggest that those genes that are differently expressed in response to *PuHSFA4a* expression are independent of both previously defined Zn stress response genes and known *HSFA4a* target genes found in *P. ussuriensis* roots. Further functional study of downstream genes will help to clarify this issue.

The antioxidative enzyme GST was reported to play an important role in abiotic stress resistance by reducing ROS toxicity (Jiang and Yan, 2018). In *Juglans regia*, overexpression of *JrGSTTau1* confers chilling stress tolerance by decreasing ROS accumulation and thereby reducing cell damage (Yang et al., 2016). Ectopic expression of rice *OsGSTU4* improves tolerance to salinity and oxidative stresses in Arabidopsis by enhancing GST activity, thereby suppressing ROS accumulation (Sharma et al., 2014). In our study, a tau class PuGST (PuGSTU17), homologous to Arabidopsis AtGSTU17, was identified as a direct target of PuHSFA4a by RT-qPCR, ChIP-qPCR, Y1H, and LUC assays, and by EMSA. Furthermore, ROS accumulation was significantly decreased in *PuGSTU17* overexpressing lines but obviously increased in the *PuGSTU17*-RNAi lines compared with wild type under excess Zn. Accordingly, overexpression of *PuHSFA4a* significantly increased GST activity in roots under excess Zn, while a dominant repressor version of *PuHSFA4a* decreased GST activity. Taken together, our results demonstrate that PuHSFA4a can activate the target gene *PuGSTU17* to promote GST activity to eliminating excess Zn-induced ROS in roots and thereby improve Zn tolerance. This finding agrees with previous studies showing that overexpression of tau GSTs from *Pyrus pyrifolia* increased tolerance to Cd (Liu et al., 2013), tau GSTs from *Gly soja* and *Salicornia brachiata* enhanced salt tolerance, and tau GSTs from *G. soja* improved drought tolerance in tobacco (*Nicotiana benthamiana*; Ji et al., 2010; Jha et al., 2011). However, we found that both *PuHSFA4a* and *PuGSTU17* overexpression specifically improves plant resistant to excess Zn but does not confer tolerance to some other heavy metal stresses. In this regard, the relationship between *PuHSFA4a* and *PuGSTU17* under Zn stress remains to be clarified.

The developmental plasticity of root shape is important for root function and plant survival after exposure to toxic heavy metals (Lin and Aarts, 2012). PLA enzymatic hydrolysate free fatty acids were reported to be second messengers that are involved in auxin functions such as activation of elongation and cell division (Holk and Scherer, 1998). In previous studies, PLA was identified as a regulator of plant growth and development (Wang et al., 2000; Holk et al., 2002; La Camera et al., 2005; Schvartzman et al., 2018). For instance, Arabidopsis *AtPLAIVA*-null mutants have reduced lateral root development by reduced auxin signaling (Schvartzman et al., 2018). In this study, ChIP-qPCR, Y1H, and LUC assays and EMSA confirmed that $PuPLA_2$ was also a direct target gene of *PuHSFA4a* (Fig. 7; Supplemental Fig. S6). Under excess Zn, both the $PuPLA_2$-OE and *PuHSFA4a*-OE lines displayed similar phenotypes with respect to root growth compared to wild-type plants. In addition, *PuPIF3* expression was upregulated by both *PuHSFA4a* overexpression and $PuPLA_2$ overexpression under excess Zn conditions. Previous studies reported that PIFs are involved in the regulation of auxin signaling and auxin biosynthesis in plants. For instance, Arabidopsis PIF3 lies downstream of PHYB and RGL3, and has been shown to reduce the inhibitory effect of nitric oxide on root growth in Arabidopsis (Bai et al., 2014). Arabidopsis PIF4 also regulates hypocotyl growth by directly targeting the auxin biosynthesis gene *YUCCA8* and the auxin signaling gene *IAA29* (Sun et al., 2012, 2013), and regulates root growth by modulating the expression of the auxin biosynthesis genes *TAA1* and *CYP79B2* in response to high temperatures (Franklin et al., 2011). These results suggest that PuHSFA4a might confer excess Zn tolerance partly by regulating $PuPLA_2$ to promote the expression of PIF3 and thereby influencing the auxin signaling pathway, thus contributing to root growth. Further elucidation of the mechanisms underlying PuHSFA4a regulation of $PuPLA_2$ and *PuPIF3* expression under Zn stress should be a focus of future work.

Based on our findings, we propose a model of action for *PuHSFA4a* in response to excess Zn in roots (Fig. 10).

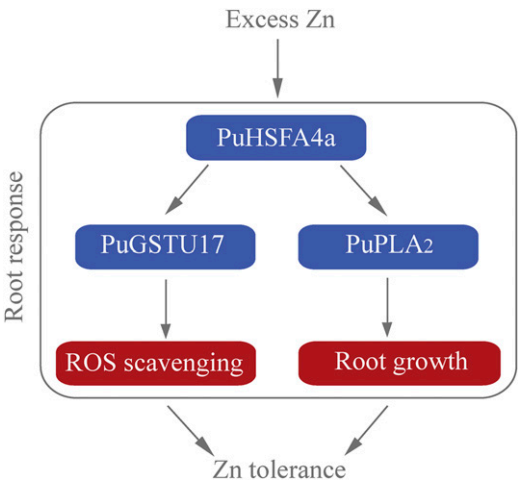

Figure 10. A proposed model illustrating excess Zn tolerance regulated by the PuHSFA4a. PuHSFA4a is induced by high Zn content in *P. ussuriensis* roots. Under excess Zn stress, *PuHSFA4a* activates *PuGSTU17* expression by binding with its promoters, followed by enhancing GST activity, which resulted in enhancing tolerance by reducing ROS. Meanwhile, overexpression of *PuHSFA4a* promotes root growth by directly binding with the $PuPLA_2$ promoter to activate its transcription under Zn stress. Thus, PuHSFA4a functions as a positive regulator of excess Zn tolerance by activating the antioxidant system and promoting root growth in *P. ussuriensis*.

In this article, we have provided evidence that the root-specific–induced gene *PuHSFA4a* positively regulates high Zn tolerance in roots of *P. ussuriensis* by coordinately activating the antioxidant system and root development genes and that it directly targets *PuGSTU17* and *PuPLA*$_2$. This study thus identifies PuHSFA4a as a positive and specific regulator of excess Zn tolerance in *P. ussuriensis* and provides insight into the mechanisms of excess Zn tolerance in *Populus* roots.

MATERIALS AND METHODS

Plant Materials and Growth Conditions

Populus ussuriensis clone Donglin plants were grown in vitro under 16-h–light/8-h–dark cycles at 46 μmol photons m^{-2} s^{-1} irradiation at 25°C. Plants were grown on half-strength MS plates with 0.6% (w/v) agar and 2% (w/v) Suc for two weeks followed by culturing on a medium supplemented with 1.2 mM of $ZnSO_4$ for 0, 3, 6, 12, 24, 48 h, and 1 week, respectively. The plants were also exposed to 80 μM of $CdCl_2$, 100 μM of $CuSO_4$, 1.0 mM of $FeSO_4$, 7% (w/v) PEG6000, 30 μM of ABA, and 150 mM of NaCl treatments for 0, 12, and 24 h, respectively. At the end of the experimental period, leaf and root tissues were collected, frozen in liquid nitrogen, and stored at −80°C. For gene expression and physiology analysis, plants were grown in a growth chamber at 25°C, in a 16-h–light,/8-h–dark photoperiod with a light intensity of 46 μmol photons m^{-2} s^{-1}.

RNA Extraction and RT-qPCR Analysis

Total RNA was extracted using the cetyltrimethylammonium bromide method (Zhang et al., 2015), and reverse-transcription was performed using the PrimeScript RT First Strand cDNA Synthesis Kit (Toyobo). First-strand cDNA synthesized from 0.5 μg of purified RNA was reverse-transcribed using a Reverse Transcriptase Kit (TaKaRa). RT-qPCR was performed with primers corresponding to sequences from the UniGene database developed from a nonparametric RNA-seq of *P. ussuriensis*. RT-qPCR was carried out using a TransStart Top Green qPCR SuperMix (TransGen Biotech) with PCR conditions following the manufacturer's instructions. We also used a qTOWER 3G Cycler and qPCR software (Analytik) to perform RT-qPCR and analyze data. The *P. ussuriensis Actin* (*PuActin*) gene was used as an internal control. The $2^{-\Delta\Delta Ct}$ method was used to determine the relative abundance of transcripts. All primers used in this study are listed in Supplemental Table S5.

Phylogenetic Analysis and Protein Domain Identification

The HSF proteins were searched against the NCBI database (http://www.ncbi.nlm.nih.gov/). A phylogenetic tree was constructed based on HSF amino acid sequences using the neighbor-joining method in the software MEGA v5.0 (Tamura et al., 2011) and a bootstrap test with 1,000 iterations. Multiple sequence alignment of the full-length protein sequences was performed using the software BioEdit v7.1 (Hall, 1999).

Generation of Transgenic Plants

A 2,203-bp genomic promoter sequence upstream of the coding region of *PuHSFA4a* was cloned into a pCAMBIA1301 binary vector instead of the cauliflower mosaic virus 35S promoter. The full-length coding sequences (CDSs) of *PuHSFA4a* and *PuGSTU17* were amplified by PCR and cloned into the pBI121 vector containing the cauliflower mosaic virus 35S promoter to generate the 35S::*PuHSFA4a* and 35S::*PuGSTU17* constructs, respectively. A 27-bp DNA sequence encoding the *SRDX* repression domain (Chai et al., 2014) was fused in-frame to the 3′ end of the *PuHSFA4a* coding regions and then cloned into the pBI121 vector to generate the 35S::*PuHSFA4a-SRDX* constructs, respectively. The coding region of the *PuPLA*$_2$ gene was cloned into a pCAMBIA1300 vector. For the *PuGSTU17* RNAi construct, a 179-bp specific fragment beginning with an ATG starting at base 507 and ending at base 685 from *PuGSTU17* was PCR-amplified using primers *PuGSTU17*-RNAi-F and *PuGSTU17*-RNAi-R. The resulting PCR product was cloned into a pENTR vector (Invitrogen) and was subsequently transferred into the RNAi destination vector pH7GWIWG2(II); Karimi et al., 2005). The vectors constructed included ProPuHSFA4a::*GUS*, 35S::*PuHSFA4a-GFP*, 35S::*PuHSFA4a-SRDX-GFP*, 35S::*PuGSTU17-GFP*, *PuGSTU17*-RNAi, and 35S::*PuPLA*$_2$*-GFP*. These were introduced into *Agrobacterium* strain EHA105 before transformation by leaves. Transformants were selected on media containing 40 mg L^{-1} kanamycin except ProPuHSFA4a::*GUS*, *PuGSTU17*-RNAi, and *PuPLA*$_2$-OE plants, which were selected on media containing 4.0 mg L^{-1} hygromycin. All transgenic plants were confirmed by genomic PCR and by RT-qPCR. At least 10 transgenic lines were used for phenotypic observations. From these lines, data were obtained from four or more transgenic lines that showed a common and stable phenotype. All primer sequences used in this study are listed in Supplemental Table S5.

Abiotic Stress and Zinc Tolerance Assays

Seven-day–old in vitro plants (wild type, *PuHSFA4a*-OE, *PuHSFA4a-SRDX*, *PuGSTU17*-OE, *PuGSTU17*-RNAi, and *PuPLA*$_2$-OE) were transferred to half-strength MS medium containing 1.2 mM of $ZnSO_4$, 70 μM or 80 μM of $CdCl_2$, 100 μM of $CuSO_4$, 1.0 mM of $FeSO_4$, 7% (w/v) PEG6000, 30 μM of ABA, and 150 mM of NaCl for 2 weeks, respectively, unless otherwise specified. In addition, 2-month–old soil grown plants were irrigated with 5.0 mM of $ZnSO_4$ for four weeks under the same light regime in soil. In a preliminary experiment, we evaluated the effect of different concentrations of $ZnSO_4$ on in vitro and soil grown *P. ussuriensis*. The results showed that 1.2-mM and 5-mM Zn concentrations could reduce but not abolish in vitro and soil grown *P. ussuriensis*, respectively. Thus, 1.2-mM and 5-mM Zn concentrations were used as moderate excess Zn stress treatment for in vitro and soil grown plants in this study, respectively.

Measurement of EL, MDA Content, ROS Accumulation, and GST Activity

Seven-day–old in vitro plants were cultured on half-strength MS medium with or without 1.2 mM of $ZnSO_4$, respectively. After 2 weeks of culture, the roots were collected and used for analysis.

MDA content was quantified as described by Metwally et al. (2003). About 50 mg of roots were ground in liquid nitrogen and homogenized in 1 mL of 0.1% (w/vTCA for 10 min and centrifuged at 10,000*g* for 15 min at 4°C. A quantity of 0.2 mL of the supernatant was reacted with 0.8 mL of 20% (w/v) TCA containing 0.5% (w/v) thiobarbituric acid. The mixture was boiled for 20 min and cooled immediately, then centrifuged at 10,000*g* for 5 min at 4°C. The absorbance of the supernatant was measured in 532 and 600 nm, respectively. The concentration of MDA was calculated using the extinction coefficient of 155 mmol^{-1} L^{-1} cm^{-1} and expressed as nmol g^{-1} fresh weight (Hossain et al., 2017).

Measurements of EL were performed as described in Duan et al. (2017) with some modifications. Briefly, three entire roots were immersed in 150-mL tubes containing 80 mL of deionized water. After 15 min of vacuum treatment and shaking at 140 rpm for 2 h at room temperature, the conductivities (C1) were determined with an electrical conductivity meter (DDS-307A; Hinotek). The samples were then boiled for 15 min. After cooling to 25°C, the conductivities of the roots (C2) and deionized water (C0) were determined again. The relative ion leakage% = (C1-C0) / (C2-C0)*100% was subsequently calculated.

For histochemical detection of H_2O_2 accumulation, the roots were treated with 3, 3′-diaminobenzidine (DAB) solutions (1.0 mg mL^{-1} DAB-HCl at pH 3.8; Sigma-Aldrich; Zhang et al., 2014). The stained roots were bleached in acetic acid-ethanol (1:3, v/v) solution at 25°C for 3 h, and then stored in a glycerol-ethanol (1:4, v/v) solution. Pictures were taken with SZ Stereo Microscopes (Olympus).

H_2O_2 was quantified by chemiluminescence (CL) with luminol as described by König et al. (2014). About 100 mg of roots were pulverized with a mortar and pestle in liquid nitrogen, and then mixed with 0.5 mL of 5% (w/v) TCA at 4°C. The samples were placed in the dark for 40 min and centrifugated at 10,000*g* for 10 min at 4°C. After dilution with 0.1-M sodium carbonate buffer, 50-μL aliquots were incubated with 100 U of catalase (bovine liver; Sigma-Aldrich) or with the same volume of water for 30 min at 30°C as a control. H_2O_2 was determined by CL with luminol. The sample (5 μL) was added to 100 μL of reagent solution. The emitted photons were counted over 7 s with a Synergy H1 Hybrid Multi-Mode Microplate Reader (BioTek). The difference between catalase-treated and untreated samples (ΔCL) was considered as H_2O_2-specific CL. A standard curve was generated using appropriate dilutions of 30% (w/v) H_2O_2 (Farooq et al., 2016).

For detection of GST activity, frozen roots were ground in a liquid-nitrogen prechilled mortar containing 50 mM of phosphate-buffered saline at pH 7.2, 1 mM of EDTA, 8% (w/v) polyvinylpolypyrrolidone, 2 mM of DTT, and 0.01% (v/v) Triton 100-X. The extract was passed through Miracloth and then centrifuged at 23,000*g* for 30 min at 4°C (Davoine et al., 2006). The supernatants were used for GST activity analysis by using a GST (glutathione-ST) Assay Kit (Nanjing Jiancheng Bioengineering Institute) according to the manufacturer's instructions. The total proteins in the samples were quantified by using a Bradford Protein Assay Kit (Solarbio) according to the manufacturer's instructions.

Chlorophyll and Zn Content Analyses

Two-month-old soil grown plants were irrigated with or without 5.0 mM of $ZnSO_4$ for 4 weeks.

The third leaf was collected for measurements of chlorophyll and the whole roots were collected for measurements of Zn content, respectively.

For total chlorophyll quantification, ~20–30 mg leaves were ground in liquid nitrogen and thoroughly mixed with 2.5 mL of 80% (v/v) acetone by vigorous vortexing. The samples were then incubated in darkness overnight at 4°C. The mixtures were centrifuged at 10,000*g* for 20 min at 4°C. The absorbance of supernatant was measured at 663 and 645 nm (Porra, 2002). Total chlorophyll content was calculated and expressed as mg g^{-1} fresh weight.

The concentration of Zn in roots was analyzed as described by Cho et al. (2003) with some modifications. The roots were harvested, briefly washed using deionized water, and dried at 60°C until their weights remained constant. About 500 mg of dry homogeneous sample was digested with 5-mL 65% (v/v) HNO_3 at 150°C until complete solubilization of the sample occurred. The cleared extracts were then diluted with ultra-pure water to 25 mL and analyzed by inductively coupled plasma optical emission spectrometry (Agilent Technologies).

Histochemical GUS Staining

Histochemical GUS-staining assays were performed as described in Jefferson et al. (1987) with minor modifications. Two-week–old Pro-PuHSFA4a::*GUS* plants were treated with or without $ZnSO_4$ (1.2 mM) for 7 d. After this treatment all plants were incubated in a solution for ~16 h at 37°C in 100 mM of sodium P buffer (pH 7.0) containing 0.6 g of 5-bromo-4-chloro-3-indolyl-β-D-GlcA cyclohexylammonium salt, 5 mM of potassium ferrocyanide, 5 mM of potassium ferricyanide, 0.1 M of EDTA disodium salt, and 0.1% (v/v) Triton X-100. Tissues were fixed with fixative solution (glacial acetic acid-absolute ethanol, 1:3 [v/v]) and then immersed in transparent solution (glycerin-absolute ethanol, 1:4). GUS activity was imaged using at least three replicates.

Subcellular Localization and Transcriptional Activation of *PuHSFA4a*

Subcellular localization was performed by expressing 35S::*GFP* and 35S::*PuHSFA4a-GFP* in onion (*Allium cepa*) tissue epidermal cells via a biolistic bombardment method (Lee et al., 2008). GFP fluorescent signals for the fusion protein were examined with a LSM 710 Meta confocal microscope (Zeiss) at an excitation wavelength of 488 nm and an emission wavelength of 509 nm. Plasma membrane localization was confirmed by plasmolysis after onion epidermal cells were treated with 30% (w/v) Suc solution for 20 min. To estimate PuHSFA4a transcriptional activation, full-length and six partial CDSs of the *PuHSFA4a* gene were cloned into the *Nco*I and *Sal*I sites of the pGBKT7 vector to fuse with the GAL4 DBD (Aoyama and Chua, 1997). The vector was then transformed into the yeast strain AH109 (Clontech). The transformed yeast was spread on SD/-Trp, SD/-Trp/X-α-Gal, and SD/-Trp/-His/-Ade media (Coolaber) and incubated at 30°C for 3–5 d. The negative control, a pGBKT7 empty vector in AH109, was treated the same way. The primer sequences for vector construction and six partial CDSs are shown in Supplemental Table S5.

Protein Extraction from Transgenic Lines and Immunoblot Analysis

35S::*GFP* and 35S::*PuHSFA4a-GFP* reporter constructs were transiently expressed in *P. ussuriensis* leaves as described in Takata and Eriksson (2012). Total proteins were extracted from infected leaves expressing either GFP or PuHSFA4a fused with GFP using protein extraction buffer (10 mM of Tris-Cl at pH 7.5; 150 mM of NaCl; 0.5 mM of EDTA; 1 mM of phenylmethanesulfonyl fluoride; 0.5% [w/v] Nonidet P-40). We detected GFP and PuHSFA4a-GFP protein abundance by using a rabbit anti–GFP antibody (Abcam) and a goat anti-rabbit IgG H&L (HRP; ab205718; Abcam) secondary antibody. Immunoreactive polypeptides were visualized by using the western ECL blotting substrate BeyoECL Moon (Beyotime). Imaging was performed using a model no. LAS-4000 Imaging System (Fijifilm).

Transcriptome Analysis

To assess *PuHSFA4a*-mediated excess Zn tolerance in *P. ussuriensis* using RNA-seq experiments, in vitro cuttings of *PuHSFA4a*-OE and wild type were grown for 7 d in half strength MS medium, and were then transferred to half strength MS medium supplemented with 1.2 mM of $ZnSO_4$ for two weeks. A separate cohort of plants was grown in half strength MS medium for all three weeks as a control. Total RNA isolation, library construction, and sequencing were performed by Anoroad Technologies. In total, 2 μg RNA was prepared for library construction. Sequencing was performed on a HiSeq 4000 (Illumina). Obtained reads were mapped to the *P. trichocarpa* genome (http://phytozome.jgi.doe.gov) using the software TopHat2 (http://ccb.jhu.edu/software/tophat/index.shtml; Kim et al., 2013), differential expression analysis was conducted using the programs Cuffdiff (http://cole-trapnell-lab.github.io/cufflinks/) and DEseq2 (https://bioconductor.org/packages/release/bioc/html/DESeq2.html; Love et al., 2014). Heatmaps were generated using the software GENE (https://software.broadinstitute.org/GENE-E/). Ontology enrichment was analyzed using the software BiNGO (https://www.psb.ugent.be/cbd/papers/BiNGO/Home.html). Finally, our RNA-seq results were verified by RT-qPCR and all primers used are shown in Supplemental Table S5.

ChIP Assays

In vitro cuttings of *PuHSFA4a*-OE and wild type were grown for 7 d in half strength MS medium, and were then transferred to 1/2 MS medium supplemented with or without 1.2 mM of $ZnSO_4$ for 2 weeks. Then, the roots of *PuHSFA4a*-OE transgenic plants were harvested for analysis using ChIP-PCR (Li et al., 2014) and ChIP-qPCR (Huang et al., 2017). GFP antibodies (Beyotime) bound to Protein-A agarose beads (Sigma-Aldrich) were used for the ChIP assays. A rabbit anti-hemagglutinin antibody was used as a negative control (Mock), and *PuActin* was used as a control. The degree of enrichment of promoter fragments over 13 genomic fragments were determined by PCR and RT-qPCR. The primers used for these analyses are listed in Supplemental Table S5.

Y1H Assays

The promoters of *PuGSTU17* (1,654-bp) and $PuPLA_2$ (1,673-bp) were PCR-amplified and inserted into a pAbAi-BR yeast integrating vector (bait–reporter; Clontech) and the *PuHSFA4a* gene was cloned into the pGADT7-rec vector (Clontech) in frame with the GAL4 activation domain. The pGADT7-*PuHSFA4a* and pAbAi-*ProPuGSTU17* or pGADT7-*PuHSFA4a* and pAbAi-*ProPuPLA*$_2$ vectors were cotransformed into yeast Y1HGold strain using a Matchmaker One-Hybrid Library Construction and Screening Kit (Clontech). Cotransformed yeast cells were selected on SD/-Ura-Leu (a synthetic dropout medium lacking Ura and Leu) with or without AbA (0.6 mg L^{-1}; Sigma-Aldrich), and were then incubated for 3–5 d at 30°C. The Y1H assay was conducted as described in Wang et al. (2014). Both positive (pGAD-p53+p53-pAbAi) and negative (pGADT7-AD+ProPuGSTU17-pAbAi or ProPuPLA$_2$-pAbAi) controls were carried out in the same manner. The primers used for these analyses are listed in Supplemental Table S5.

Dual LUC Assay

The promoters of *PuGSTU17* (1,654 bp) and $PuPLA_2$ (1,673 bp) were cloned into pGreenII0800-LUC vectors as reporters. Full-length open reading frames of *PuHSFA4a* were cloned into pBI121-*GFP* vectors as the effector. The effector and reporter vectors were cotransformed into leaves of *Nicotiana benthamiana* as previously described by He et al. (2013). Detection of dual LUC activity was also carried out according to He et al. (2013). A Synergy H1 Microplate Reader (Bio-Tek) and a Dual-Luciferase Assay Kit (Promega) were used to detect the firefly LUC and Renilla luciferase activities according to the manufacturer's instructions. The primers used for these analyses are listed in Supplemental Table S5.

EMSA

The full-length CDS of *PuHSFA4a* was inserted into vector pET32a (Novagen) for production of recombinant PuHSFA4a protein in *Escherichia coli* BL21. Transformed *E. coli* were then grown in liquid media to an OD600 nm of 0.5, treated with 0.6 mM of isopropyl-b-D-thiogalactopyranoside for 7 h at 30°C, and then collected by centrifugation. The His-PuHSFA4a fusion protein was purified using PureCube Ni-NTA Agarose (Cube Biotech). The probes were labeled with biotin using an EMSA Probe Biotin Labeling Kit (Beyotime) with all procedures performed as per the manufacturer's instructions, and an unlabeled probe was used as the competitor. EMSA was conducted using a Chemiluminescent EMSA Kit (Beyotime). Reactions were incubated at 25°C for 30 min after the addition of 2 μg of protein from the His purification eluate. Four probes were generated for *PuGSTU17* and *PuPLA*$_2$ promoters using the same oligonucleotides described in Supplemental Table S5.

Statistical Analysis

Stress treatments were repeated at least three times. The statistical significance between two means (except for microarray data) was determined using ANOVAs followed by posthoc *t* tests to examine pairwise differences. All tests were reported such that asterisks indicated a significance level of $P < 0.05$ and ** indicated $P < 0.01$.

Accession Numbers

Nucleic acid sequences of *PuHSFA4a*, *PuGSTU17*, and *PuPLA*$_2$ from *P. ussuriensis* have been deposited into GenBank with accession numbers of MH668277, MH668278, and MH668279. The raw sequence data of RNA-seq experiments reported in this study have been deposited in the Gene Expression Omnibus with accession numbers of GSE117778.

Supplemental Data

The following supplemental materials are available.

Supplemental Figure S1. RT-qPCR analysis of Class A of HSFs expression under Zn stress and *PuHSFA4a* and *PuGSTU17* expression under abiotic stresses.

Supplemental Figure S2. Immunoblot analysis used anti-GFP antibody to verify PuHSFA4a-GFP fusion protein expression.

Supplemental Figure S3. Phenotypes and RT-qPCR confirmation of *PuHSFA4a*-overexpression (*A4a*-OE3 and *A4a*-OE8) and a dominant repressor version of *PuHSFA4a* (*A4a-SRDX*1 and *A4a-SRDX*6) *P. ussuriensis* plants.

Supplemental Figure S4. Phenotypes of wild type, *PuHSFA4a*-overexpression (*PuHSFA4a*-OE), and *PuHSFA4a*-suppression (*PuHSFA4a-SRDX*) transgenic *P. ussuriensis* plants under various abiotic stresses.

Supplemental Figure S5. Gene Ontology categorization of PuHSFA4a-binding genes under excess Zn stress.

Supplemental Figure S6. ChIP-PCR analysis of PuHSFA4a binding to *PuGSTU17* and *PuPLA*$_2$ gene promoters.

Supplemental Figure S7. Phenotypes and RT-qPCR confirmation of *PuGSTU17*-overexpression (*PuGSTU17*-OE) and *PuGSTU17* suppression (*PuGSTU17*-RNAi) in *P. ussuriensis*.

Supplemental Figure S8. Phenotypes of wild-type and *PuGSTU17*-overexpression (*PuGSTU17*-OE) transgenic *P. ussuriensis* plants under different abiotic stresses.

Supplemental Figure S9. RT-qPCR analysis to confirm *PuPLA*$_2$-overexpression transgenic lines and phenotypic observation of plants.

Supplemental Table S1. DEGs in wild-type *P. ussuriensis* plants with or without excess Zn stress ($\log_2$ Fold Change > 1, P value < 0.01).

Supplemental Table S2. DEGs in *PuHSFA4a*-overexpression (*PuHSFA4a*-OE) transgenic *P. ussuriensis* plants with or without excess Zn stress ($\log_2$ Fold Change > 1, P value < 0.01).

Supplemental Table S3. DEGs between wild-type and *PuHSFA4a*-overexpression (*PuHSFA4a*-OE) transgenic *P. ussuriensis* plants under control conditions ($\log_2$ Fold Change > 1, P value < 0.01).

Supplemental Table S4. DEGs between wild-type and *PuHSFA4a*-overexpression (*PuHSFA4a*-OE) transgenic *P. ussuriensis* plants under excess Zn conditions ($\log_2$ Fold Change > 1, P value < 0.01).

Supplemental Table S5. Primers used in this study.

ACKNOWLEDGMENTS

We acknowledge TopEdit English Editing LLC for the linguistic editing and proofreading during the preparation of this article.

Received November 30, 2018; accepted June 11, 2019; published June 20, 2019.

LITERATURE CITED

Aoyama T, Chua NH (1997) A glucocorticoid-mediated transcriptional induction system in transgenic plants. Plant J **11:** 605–612

Ariani A, Francini A, Andreucci A, Sebastiani L (2016) Over-expression of AQUA1 in *Populus alba Villafranca* clone increases relative growth rate and water use efficiency, under Zn excess condition. Plant Cell Rep **35:** 289–301

Arrivault S, Senger T, Krämer U (2006) The Arabidopsis metal tolerance protein AtMTP3 maintains metal homeostasis by mediating Zn exclusion from the shoot under Fe deficiency and Zn oversupply. Plant J **46:** 861–879

Bai S, Yao T, Li M, Guo X, Zhang Y, Zhu S, He Y (2014) PIF3 is involved in the primary root growth inhibition of Arabidopsis induced by nitric oxide in the light. Mol Plant **7:** 616–625

Barceló J, Poschenrieder C (1990) Plant water relations as affected by heavy metal stress: A review. J Plant Nutr **13:** 1–37

Bittsánszky A, Kömives T, Gullner G, Gyulai G, Kiss J, Heszky L, Radimszky L, Rennenberg H (2005) Ability of transgenic poplars with elevated glutathione content to tolerate zinc(2+) stress. Environ Int **31:** 251–254

Blaudez D, Kohler A, Martin F, Sanders D, Chalot M (2003) Poplar metal tolerance protein 1 confers zinc tolerance and is an oligomeric vacuolar zinc transporter with an essential leucine zipper motif. Plant Cell **15:** 2911–2928

Broadley MR, White PJ, Hammond JP, Zelko I, Lux A (2007) Zinc in plants. New Phytol **173:** 677–702

Chai G, Qi G, Cao Y, Wang Z, Yu L, Tang X, Yu Y, Wang D, Kong Y, Zhou G (2014) Poplar PdC3H17 and PdC3H18 are direct targets of *PdMYB3* and *PdMYB21*, and positively regulate secondary wall formation in Arabidopsis and poplar. New Phytol **203:** 520–534

Chang H, Lin C, Huang H (2005) Zinc-induced cell death in rice (*Oryza sativa* L.) roots. Plant Growth Regul **46:** 261–266

Chaoui A, Mazhoudi S, Ghorbal MH, El Ferjani E (1997) Cadmium and zinc induction of lipid peroxidation and effects on antioxidant enzyme activities in bean (*Phaseolus vulgaris* L). Plant Sci **127:** 139–147

Chen J, Yang L, Gu J, Bai X, Ren Y, Fan T, Han Y, Jiang L, Xiao F, Liu Y, et al (2015) *MAN3* gene regulates cadmium tolerance through the glutathione-dependent pathway in *Arabidopsis thaliana*. New Phytol **205:** 570–582

Cho M, Chardonnens AN, Dietz KJ (2003) Differential heavy metal tolerance of *Arabidopsis halleri* and *Arabidopsis thaliana*: A leaf slice test. New Phytol **158:** 287–293

Davoine C, Falletti O, Douki T, Iacazio G, Ennar N, Montillet JL, Triantaphylidès C (2006) Adducts of oxylipin electrophiles to glutathione reflect a 13 specificity of the downstream lipoxygenase pathway in the tobacco hypersensitive response. Plant Physiol **140:** 1484–1493

Desbrosses-Fonrouge AG, Voigt K, Schröder A, Arrivault S, Thomine S, Krämer U (2005) *Arabidopsis thaliana* MTP1 is a Zn transporter in the vacuolar membrane which mediates Zn detoxification and drives leaf Zn accumulation. FEBS Lett **579:** 4165–4174

Duan M, Zhang R, Zhu F, Zhang Z, Gou L, Wen J, Dong J, Wang T (2017) A lipid-anchored NAC transcription factor is translocated into the nucleus and activates glyoxalase I expression during drought stress. Plant Cell **29:** 1748–1772

Farooq MA, Detterbeck A, Clemens S, Dietz KJ (2016) Silicon-induced reversibility of cadmium toxicity in rice. J Exp Bot **67:** 3573–3585

Franklin KA, Lee SH, Patel D, Kumar SV, Spartz AK, Gu C, Ye S, Yu P, Breen G, Cohen JD, et al (2011) Phytochrome-interacting factor 4 (PIF4) regulates auxin biosynthesis at high temperature. Proc Natl Acad Sci USA **108:** 20231–20235

Garg N, Kaur H (2013) Response of antioxidant enzymes, phytochelatins and glutathione production towards Cd and Zn stresses in *Cajanus cajan* (L.) Millsp. genotypes colonized by arbuscular mycorrhizal fungi. J Agron Crop Sci **199:** 118–133

Gong B, Yi J, Wu J, Sui J, Khan MA, Wu Z, Zhong X, Seng S, He J, Yi M (2014) LlHSFA1, a novel heat stress transcription factor in lily (*Lilium longiflorum*), can interact with LlHSFA2 and enhance the thermotolerance of transgenic *Arabidopsis thaliana*. Plant Cell Rep **33:** 1519–1533

Hall TA (1999) BioEdit: A user-friendly biological sequence alignment editor and analysis program for Windows 95/98/NT. Nucleic Acids Symp Ser **41:** 95–98

Han Y, Sa G, Sun J, Shen Z, Zhao R, Ding M, Deng S, Lu Y, Zhang Y, Shen X (2014) Overexpression of *Populus euphratica* xyloglucan endo transglucosylase/hydrolase gene confers enhanced cadmium tolerance by the restriction of root cadmium uptake in transgenic tobacco. Environ Exp Bot **100:** 74–83

He J, Li H, Luo J, Ma C, Li S, Qu L, Gai Y, Jiang X, Janz D, Polle A, et al (2013) A transcriptomic network underlies microstructural and physiological responses to cadmium in *Populus* × *canescens*. Plant Physiol **162:** 424–439

Holk RUPA, Scherer GF (1998) Fatty acids and lysophospholipids as potential second messengers in auxin action. Rapid activation of phospholipase A_2 activity by auxin in suspension-cultured parsley and soybean cells. Plant J **16:** 601–611

Holk A, Rietz S, Zahn M, Quader H, Scherer GF (2002) Molecular identification of cytosolic, patatin-related phospholipases A from Arabidopsis with potential functions in plant signal transduction. Plant Physiol **130:** 90–101

Hossain MS, ElSayed AI, Moore M, Dietz KJ (2017) Redox and reactive oxygen species network in acclimation for salinity tolerance in sugar beet. J Exp Bot **68:** 1283–1298

Hu S, Wang XC, Yang JY (2013) [Interannual variation patterns of heavy metals concentrations in tree rings of *Larix gmelinii* near Xilin lead–zinc mine, Yichun of Northeast China]. Ying Yong Sheng Tai Xue Bao **24:** 1536–1544

Huang X, Zhang X, Gong Z, Yang S, Shi Y (2017) ABI4 represses the expression of type-A ARRs to inhibit seed germination in Arabidopsis. Plant J **89:** 354–365

Jefferson RA, Kavanagh TA, Bevan MW (1987) GUS fusions: β-glucuronidase as a sensitive and versatile gene fusion marker in higher plants. EMBO J **6:** 3901–3907

Jha B, Sharma A, Mishra A (2011) Expression of *SbGSTU* (tau class glutathione s-transferase) gene isolated from *Salicornia brachiata* in tobacco for salt tolerance. Mol Biol Rep **38:** 4823–4832

Ji W, Zhu Y, Li Y, Yang L, Zhao X, Cai H, Bai X (2010) Over-expression of a glutathione s-transferase gene, *GsGST*, from wild soybean (*Glycine soja*) enhances drought and salt tolerance in transgenic tobacco. Biotechnol Lett **32:** 1173–1179

Jiang D, Yan S (2018) Effects of Cd, Zn, or Pb stress in *Populus alba* berolinensis on the antioxidant, detoxifying, and digestive enzymes of *Lymantria dispar*. Environ Entomol **47:** 1323–1328

Karimi M, De Meyer B, Hilson P (2005) Modular cloning and expression of tagged fluorescent protein in plant cells. Trends Plant Sci **10:** 103–105

Khare D, Mitsuda N, Lee S, Song WY, Hwang D, Ohme-Takagi M, Martinoia E, Lee Y, Hwang JU (2017) Root avoidance of toxic metals requires the GeBP-LIKE 4 transcription factor in *Arabidopsis thaliana*. New Phytol **213:** 1257–1273

Kim D, Pertea G, Trapnell C, Pimentel H, Kelley R, Salzberg SL (2013) TopHat2: Accurate alignment of transcriptomes in the presence of insertions, deletions and gene fusions. Genome Biol **14:** R36

Kim YY, Choi H, Segami S, Cho HT, Martinoia E, Maeshima M, Lee Y (2009) AtHMA1 contributes to the detoxification of excess Zn(II) in Arabidopsis. Plant J **58:** 737–753

Kohler A, Blaudez D, Chalot M, Martin F (2004) Cloning and expression of multiple metallothioneins from hybrid poplar. New Phytol **164:** 83–93

König K, Galliardt H, Moore M, Treffon P, Seidel T, Dietz KJ (2014) Assessing redox state and reactive oxygen species in circadian rhythmicity. Methods Mol Biol **1158:** 239–271

La Camera S, Geoffroy P, Samaha H, Ndiaye A, Rahim G, Legrand M, Heitz T (2005) A pathogen-inducible patatin-like lipid acyl hydrolase facilitates fungal and bacterial host colonization in Arabidopsis. Plant J **44:** 810–825

Laity JH, Andrews GK (2007) Understanding the mechanisms of zinc-sensing by metal-response element binding transcription factor-1 (MTF-1). Arch Biochem Biophys **463:** 201–210

Lan HX, Wang ZF, Wang QH, Wang MM, Bao YM, Huang J, Zhang HS (2013) Characterization of a vacuolar zinc transporter OZT1 in rice (*Oryza sativa* L.). Mol Biol Rep **40:** 1201–1210

Lang S, Liu X, Xue H, Li X, Wang X (2017) Functional characterization of BnHSFA4a as a heat shock transcription factor in controlling the re-establishment of desiccation tolerance in seeds. J Exp Bot **68:** 2361–2375

Lee MO, Cho K, Kim SH, Jeong SH, Kim JA, Jung YH, Shim J, Shibato J, Rakwal R, Tamogami S, et al (2008) Novel rice *OsSIPK* is a multiple stress responsive MAPK family member showing rhythmic expression at mRNA level. Planta **227:** 981–990

Li F, Zhang H, Zhao H, Gao T, Song A, Jiang J, Chen F, Chen S (2018) *Chrysanthemum CmHSFA4* gene positively regulates salt stress tolerance in transgenic chrysanthemum. Plant Biotechnol J **16:** 1311–1321

Li G, Xu W, Kronzucker HJ, Shi W (2015) Ethylene is critical to the maintenance of primary root growth and Fe homeostasis under Fe stress in Arabidopsis. J Exp Bot **66:** 2041–2054

Li W, Lin YC, Li Q, Shi R, Lin CY, Chen H, Chuang L, Qu GZ, Sederoff RR, Chiang VL (2014) A robust chromatin immunoprecipitation protocol for studying transcription factor-DNA interactions and histone modifications in wood-forming tissue. Nat Protoc **9:** 2180–2193

Lin YF, Aarts MG (2012) The molecular mechanism of zinc and cadmium stress response in plants. Cell Mol Life Sci **69:** 3187–3206

Liu D, Liu Y, Rao J, Wang G, Li H, Ge F, Chen C (2013) [Overexpression of the glutathione s-transferase gene from *Pyrus pyrifolia* fruit improves tolerance to abiotic stress in transgenic tobacco plants]. Mol Biol (Mosk) **47:** 591–601

Love MI, Huber W, Anders S (2014) Moderated estimation of fold change and dispersion for RNA-seq data with DESeq2. Genome Biol **15:** 550

Luo ZB, He J, Polle A, Rennenberg H (2016) Heavy metal accumulation and signal transduction in herbaceous and woody plants: Paving the way for enhancing phytoremediation efficiency. Biotechnol Adv **34:** 1131–1148

Lyck R, Harmening U, Höhfeld I, Treuter E, Scharf KD, Nover L (1997) Intracellular distribution and identification of the nuclear localization signals of two plant heat-stress transcription factors. Planta **202:** 117–125

Metwally A, Finkemeier I, Georgi M, Dietz KJ (2003) Salicylic acid alleviates the cadmium toxicity in barley seedlings. Plant Physiol **132:** 272–281

Miyabe S, Izawa S, Inoue Y (2001) The Zrc1 is involved in zinc transport system between vacuole and cytosol in *Saccharomyces cerevisiae*. Biochem Biophys Res Commun **282:** 79–83

Morel M, Crouzet J, Gravot A, Auroy P, Leonhardt N, Vavasseur A, Richaud P (2009) AtHMA3, a P1B-ATPase allowing Cd/Zn/Co/Pb vacuolar storage in Arabidopsis. Plant Physiol **149:** 894–904

Panchuk II, Volkov RA, Schöffl F (2002) Heat stress- and heat shock transcription factor-dependent expression and activity of ascorbate peroxidase in Arabidopsis. Plant Physiol **129:** 838–853

Pérez-Salamó I, Papdi C, Gábor R, Zsigmond L, Vilela B, Lumbreras V, Nagy I, Horváth B, Domoki M, Darula Z (2014) The heat shock factor HSFA4A confers salt tolerance and is regulated by oxidative stress and the MAP kinases, MPK3 and MPK6. Plant Physiol **114:** 237891–237933

Porra RJ (2002) The chequered history of the development and use of simultaneous equations for the accurate determination of chlorophylls a and b. Photosynth Res **73:** 149–156

Schvartzman MS, Corso M, Fataftah N, Scheepers M, Nouet C, Bosman B, Carnol M, Motte P, Verbruggen N, Hanikenne M (2018) Adaptation to high zinc depends on distinct mechanisms in metallicolous populations of *Arabidopsis halleri*. New Phytol **218:** 269–282

Sharma R, Sahoo A, Devendran R, Jain M (2014) Over-expression of a rice tau class glutathione s-transferase gene improves tolerance to salinity and oxidative stresses in Arabidopsis. PLoS One **9:** e92900

Shim D, Hwang JU, Lee J, Lee S, Choi Y, An G, Martinoia E, Lee Y (2009) Orthologs of the class A4 heat shock transcription factor HsfA4a confer cadmium tolerance in wheat and rice. Plant Cell **21:** 4031–4043

Su X, Huang Q, Zhang X (2001) Study on gene resources in *Populus ussuriensis*. For Res **14:** 472–478

Sun J, Qi L, Li Y, Chu J, Li C (2012) PIF4-mediated activation of *YUCCA8* expression integrates temperature into the auxin pathway in regulating Arabidopsis hypocotyl growth. PLoS Genet **8:** e1002594

Sun J, Qi L, Li Y, Zhai Q, Li C (2013) PIF4 and PIF5 transcription factors link blue light and auxin to regulate the phototropic response in Arabidopsis. Plant Cell **25:** 2102–2114

Takahashi R, Ishimaru Y, Shimo H, Ogo Y, Senoura T, Nishizawa NK, Nakanishi H (2012) The OsHMA2 transporter is involved in root-to-shoot translocation of Zn and Cd in rice. Plant Cell Environ **35:** 1948–1957

Takata N, Eriksson ME (2012) A simple and efficient transient transformation for hybrid aspen (*Populus tremula* × *P. tremuloides*). Plant Methods **8:** 30

Tamura K, Peterson D, Peterson N, Stecher G, Nei M, Kumar S (2011) MEGA5: Molecular evolutionary genetics analysis using maximum likelihood, evolutionary distance, and maximum parsimony methods. Mol Biol Evol **28:** 2731–2739

Vaillant N, Monnet F, Hitmi A, Sallanon H, Coudret A (2005) Comparative study of responses in four Datura species to a zinc stress. Chemosphere **59:** 1005–1013

Verret F, Gravot A, Auroy P, Leonhardt N, David P, Nussaume L, Vavasseur A, Richaud P (2004) Overexpression of *AtHMA4* enhances root-to-shoot translocation of zinc and cadmium and plant metal tolerance. FEBS Lett **576:** 306–312

von Koskull-Döring P, Scharf KD, Nover L (2007) The diversity of plant heat stress transcription factors. Trends Plant Sci **12:** 452–457

Wang C, Zien CA, Afitlhile M, Welti R, Hildebrand DF, Wang X (2000) Involvement of phospholipase D in wound-induced accumulation of jasmonic acid in Arabidopsis. Plant Cell **12:** 2237–2246

Wang C, Zhang SH, Wang PF, Qian J, Hou J, Zhang WJ, Lu J (2009) Excess Zn alters the nutrient uptake and induces the antioxidative responses in submerged plant *Hydrilla verticillata* (L.f.) Royle. Chemosphere **76:** 938–945

Wang Y, Peng W, Zhou X, Huang F, Shao L, Luo M (2014) The putative *Agrobacterium* transcriptional activator-like virulence protein VirD5 may target T-complex to prevent the degradation of coat proteins in the plant cell nucleus. New Phytol **203:** 1266–1281

Xu J, Tian YS, Peng RH, Xiong AS, Zhu B, Hou XL, Yao QH (2010) *Cyanobacteria* MT gene *SmtA* enhance zinc tolerance in Arabidopsis. Mol Biol Rep **37:** 1105–1110

Xu W, Shi W, Liu F, Ueda A, Takabe T (2008) Enhanced zinc and cadmium tolerance and accumulation in transgenic Arabidopsis plants constitutively overexpressing a barley gene (*HvAPX1*) that encodes a peroxisomal ascorbate peroxidase. Botany **86:** 567–575

Yang G, Xu Z, Peng S, Sun Y, Jia C, Zhai M (2016) In planta characterization of a tau class glutathione s-transferase gene from *Juglans regia* (*JrGSTTau1*) involved in chilling tolerance. Plant Cell Rep **35:** 681–692

Zhang H, Yang J, Wang W, Li D, Hu X, Wang H, Wei M, Liu Q, Wang Z, Li C (2015) Genome-wide identification and expression profiling of the copper transporter gene family in *Populus trichocarpa*. Plant Physiol Biochem **97:** 451–460

Zhang L, Ma H, Chen T, Pen J, Yu S, Zhao X (2014) Morphological and physiological responses of cotton (*Gossypium hirsutum L.*) plants to salinity. PLoS One **9:** e112807